Journal of Plant Growth Regulation (2026) 45:3860–3882
https://doi.org/10.1007/s00344-026-12117-y

Physiological and Proteomic Shifts in *Pfaffia glomerata* Under Drought and Elevated CO_2

Tatiane Dulcineia Silva[1] · Evandro Alexandre Fortini[1] · Diego Silva Batista[2] · Kerly Jessenia Moncaleano Robledo[1] · Mariana Machado[1] · Sérgio Heitor Sousa Felipe[3] · Tadeu dos Reis de Oliveira[4] · Moab Torres de Andrade[1] · Letícia Monteiro Farias[5] · Claudete Santa-Catarina[4] · Vanildo Silveira[4] · Philipp Westhoff[6] · Andreas P. M. Weber[7] · Adriano Nunes-Nesi[1] · Wagner Campos Otoni[1]

Received: 2 December 2025 / Accepted: 11 February 2026 / Published online: 21 March 2026
© The Author(s) 2026

Abstract

Drought is a major constraint to plant growth and productivity, and rising atmospheric CO_2 concentrations are expected to modify plant responses to water limitation. However, how CO_2 enrichment reshapes the physiological, metabolic, and molecular regulation of specialized metabolite production under drought remains poorly understood. Here, we investigated the combined effects of elevated CO_2 (e[CO_2]) and drought on plant morphophysiology and on the production of 20-hydroxyecdysone (20E), a phytoecdysteroid of therapeutic relevance whose accumulation may be influenced by environmental stress, in *Pfaffia glomerata*. Plants were grown under ambient (±400 µmol mol^{-1}; a[CO_2]) or elevated (±800 µmol mol^{-1}; e[CO_2]) CO_2 concentrations combined with sufficient or limited water supply. Elevated CO_2 promoted a metabolic shift under drought, characterized by increased investment in osmoregulatory compounds, including soluble sugars, myo-inositol, and glutamate. In contrast, drought reduced photosynthetic pigments and several primary metabolites regardless of CO_2 level. Drought induced the expression of lignin biosynthesis genes (*PgC4H*, *PgCCoAOMT*, and *PgCAD*) under both CO_2 conditions; however, *PgCCR* was specifically upregulated under e[CO_2] combined with drought, with consistently higher transcript levels than under ambient CO_2. Proteomic analyses revealed that e[CO_2] attenuated the accumulation of many canonical drought-responsive proteins, while selectively promoting the accumulation of the cytochrome P450 CYP72A219-like protein, which was associated with increased whole-plant 20E production. Together, these findings show that drought drives 20E biosynthesis, while elevated CO_2 modulates drought response intensity and allocation, ultimately affecting total 20E yield per plant and its relevance under future climate scenarios.

Keywords 20-hydroxyecdysone · Drought stress · Elevated CO_2 · *Pfaffia glomerata* · Water use efficiency

Introduction

Rising atmospheric carbon dioxide concentration ([CO_2]) and increasing global temperatures are major drivers of climate change. Under pessimistic projections, [CO_2] may approach 800 ppm by the end of this century (IPCC 2014). Such enrichment profoundly influences plant metabolism, especially in C_3 species, where elevated [CO_2] (e[CO_2]) enhances RuBisCO carboxylation while suppressing oxygenase activity, thereby reducing photorespiration and increasing photosynthetic efficiency (Taub et al. 2008; Lv et al. 2022). These changes stimulate carbon assimilation and growth but also alter the coordination between carbon and nitrogen metabolism, a key determinant of plant productivity under climate change. Beyond stimulating photosynthetic performance, e[CO_2] modulates stomatal behavior, water relations, and the synthesis of primary and secondary metabolites (Qiao et al. 2010; Pazzagli et al. 2016; De la Mata et al. 2012; Houshmandfar et al. 2015; Al Jaouni et al. 2018; Almuhayawi et al. 2021; Sekhar et al. 2023).

Handling Author: Ozkan Kaya.

Extended author information available on the last page of the article

Consequently, e[CO_2] acts not merely as a photosynthetic enhancer but as a metabolic regulator that redefines resource allocation and stress adaptation in plants.

The mechanisms underlying reduced nitrogen (N) content under e[CO_2] remain debated. Decreased photorespiration may contribute, since photorespiratory flux generates amino acids such as glycine and serine, and its inhibition can disturb metabolic homeostasis (Krämer et al. 2022). e[CO_2] has also been linked to reduced nitrate (NO_3^-) assimilation, as suppressed photorespiration may lower malate transport from chloroplasts to cytoplasm, decreasing NADH production and limiting NO_3^- reduction in shoots (Bloom et al. 2020). Conversely, NO_3^- assimilation may shift from shoots to roots under e[CO_2] (Andrews et al. 2020). In *Arabidopsis thaliana* and wheat, this response depends on daytime CO_2 levels, possibly due to reduced mitochondrial respiration and slower NO_3^--to-protein conversion (Asensio et al. 2015). Additional explanations include the dilution effect, where increased biomass dilutes tissue N concentration, and restricted transpiration, which limits N translocation to shoots (Rajanayake et al. 2021). Overall, e[CO_2] modifies the C/N equilibrium and may redirect metabolic fluxes toward secondary metabolism.

Global warming driven by rising [CO_2] is also accompanied by abiotic stressors such as heat, frost, salinity, and drought (Soares et al. 2019; Mehmood et al. 2020). Drought is one of the most detrimental, limiting plant growth, pigment stability, and photosynthetic performance (Xu et al. 2016; Dusenge et al. 2019; Hatfield and Dold 2019; Iqbal et al. 2022). Under water deficit, plants show reduced net CO_2 assimilation (A_N), stomatal conductance (g_s), and transpiration rate (E), leading to decreased biomass. e[CO_2] can mitigate these effects by maintaining higher intercellular CO_2 concentrations (C_i) despite partial stomatal closure (Qiao et al. 2010; Wang et al. 2022). This adjustment improves water relations, increases water use efficiency (WUE), and supports osmotic balance. In *Coffea arabica*, for instance, e[CO_2] under drought enhances water potential and hydraulic conductance (Ávila et al. 2020). Moreover, e[CO_2] induces the accumulation of osmoregulatory solutes such as sugars and amino acids (AbdElgawad et al. 2023) and modulates antioxidant and secondary metabolite production, including alkaloids, phenols, flavonoids, terpenes, and steroids (Li et al. 2017; Hozzein et al. 2020; Roy and Mathur 2021). Abscisic acid (ABA) also plays a pivotal role in coordinating CO_2 and drought signaling by regulating stomatal closure via ABA-dependent and independent pathways (Zhang et al. 2019, 2020; Li et al. 2020; Hsu et al. 2018).

The phytoecdysteroid 20-hydroxyecdysone (20E) regulates insect development (Lin and Smagghe 2019; Guo et al. 2021) and acts in plants as a defense metabolite against herbivory (Lafont 1997; Bakrim et al. 2008). Ingestion of 20E disrupts the endocrine system of non-adapted insects, inducing premature ecdysis and mortality (Dinan et al. 2020). Owing to its bioactivity, 20E is considered both a natural insect deterrent and a compound with pharmacological benefits in humans, including anti-inflammatory, antimutagenic, and antimicrobial effects (Neves et al. 2016; Buniam et al. 2020; Dinan et al. 2021; Franco et al. 2021; Terhaag et al. 2025).

Pfaffia glomerata (Amaranthaceae), known as Brazilian ginseng, is a South American medicinal species rich in 20E (Marchioretto et al. 2010; Ribeiro et al. 2024). Its 20E content can be modulated by in vitro conditions (Iarema et al. 2012; Saldanha et al. 2013; Corrêa et al. 2015; Silva et al. 2019, 2020, 2021; Fortini et al. 2023). However, the molecular basis of 20E biosynthesis under environmental stress remains unclear (Tsukagoshi et al. 2016). Cytochrome P450 genes are central to ecdysteroid biosynthesis (Batista et al. 2019a; Janeczko et al. 2021), and *P. glomerata* possesses orthologs of the *Halloween* genes *Spook* and *Phantom*, which are upregulated under UV-B and salinity (Batista et al. 2019a; Felipe et al. 2019a, b). In *Panax ginseng*, P450 enzymes also mediate ginsenoside production (Han et al. 2011, 2019; Li et al. 2021; Choi et al. 2022; Lei et al. 2023).

Given that [CO_2] enrichment in vitro alters morphophysiological traits in *P. glomerata* (Saldanha et al. 2013, 2014; Ferreira et al. 2019; Louback et al. 2021) and that 20E accumulation is enhanced by abiotic stress (Felipe et al. 2019a, b; Fortini et al. 2023), we hypothesized that e[CO_2] interacts with drought to reprogram carbon and nitrogen metabolism, integrating primary and secondary metabolic pathways. This reprogramming is expected to promote osmotic adjustment and antioxidant responses while activating P450-mediated routes leading to 20E biosynthesis. The present study evaluates how e[CO_2] and drought interact to regulate physiological, proteomic, and metabolic responses in *P. glomerata*, identifying the cytochrome P450 CYP72A219-like protein as a potential control point linking carbon reallocation and secondary metabolism. By revealing how e[CO_2] modulates drought-induced metabolic plasticity, our findings provide mechanistic insight into how future atmospheric conditions may shape the production of specialized metabolites in medicinal plants.

Materials and Methods

Plant Material and Experimental Design

P. glomerata plants (accession number 22) were obtained from the Germplasm Bank of the Plant Tissue Culture Laboratory (LCT-II, BIOAGRO, Universidade Federal de

Viçosa). Voucher material was deposited at the Leopoldo Krieger Herbarium (UFJF, Juiz de Fora, MG, Brazil) under code number CESJ 63317. Access to genetic material (permission number AA2A367) was granted by the Brazilian National System for the Management of Genetic Heritage and Associated Traditional Knowledge (SISGEN) following existing Brazilian biodiversity legislation.

Nodal segments (1.5 cm) without leaves were cultured in vitro on MS medium with vitamins (Murashige and Skoog 1962; Powder mixture M519, Phytotech Labs), without casein hydrolysate or growth regulators, and supplemented with 3% (w/v) sucrose. The medium was solidified with 0.55% (w/v) micropropagation-grade agar (Agar Plant TC, Phytotech Labs). Culture flasks were sealed with polypropylene lids fitted with two 10-mm holes covered by 0.45-µm hydrophobic Fluoropore™ membranes, ensuring a CO_2 exchange rate of 25 µL L^{-1} s^{-1} (Batista et al. 2017). Cultures were maintained at 25 ± 2 °C, under 60 µmol m^{-2} s^{-1} irradiance (SMD 100 LED lamps, 18 W; Vilux), with a 16-h photoperiod for 30 days.

After in vitro culture, the plants were acclimatized for 7 days in 300-mL plastic cups (COPOBRAS, São Ludgero, SC, Brazil). Then, they were transplanted into plastic pots with 2 kg of commercial substrate Tropstrato HT® (Vida Verde, Mogi Mirim, SP, Brazil) and grown in a greenhouse at 21/12 ± 2 °C (day/night), with naturally fluctuating air humidity and photosynthetic photon flux density (PPFD) for another 7 days. Subsequently, plantlets were transferred to open-top chambers with a diameter of 1.15 m and a height of 1.40 m and subjected to ambient CO_2 concentration (a[CO_2]) of 400 µmol mol^{-1} or elevated CO_2 concentration (e[CO_2]) of 800 µmol mol^{-1} (Fig. S1). During the first 14 days of cultivation, all plants were irrigated regularly to maintain soil water at field capacity. CO_2 fuelling was performed during the light period from 06:00 am to 6:00 pm. Cultures were checked daily for [CO_2], temperature, and humidity using portable CO_2 sensors (CO277; Akso Produtos Eletrônicos, São Leopoldo, RS, Brazil). The open-top chambers were not sealed during CO_2 application; target CO_2 concentrations were maintained by continuous injection during the light period, with daily monitoring to ensure stable atmospheric conditions.

To evaluate the influence of CO_2 enrichment together with drought stress, plants were subjected to four treatments: (I) a[CO_2] and well-watered (a[CO_2]WW); (II) e[CO_2] and well-watered (e[CO_2]WW); (III) a[CO_2] and drought (a[CO_2]D); and (IV) e[CO_2] and drought (e[CO_2]D). Plants in treatments I and II were irrigated daily until the end of the experiment, whereas irrigation was completely suspended for plants in treatments III and IV. During greenhouse cultivation (21 days of acclimation plus 20 days of experimentation), the plants were fertilized on days 1 and 15 with 5.5 g NPK at 15:9:12 plus micronutrients (Osmocote® Plus; ICL, São Paulo, SP, Brazil). The experiment was conducted during the winter, from June to August 2021.

The experiment followed a completely randomized design based on a 2 × 2 factorial scheme, corresponding to two [CO_2] levels (ambient and elevated) and two water regimes (well-watered and drought). Each treatment consisted of one open-top chamber with fifteen biological replicates ($n = 15$). Measurements were performed on distinct samples (biological replicates), and the study was unpaired. The evaluation began when at least 50% of the plants in treatment III reached a water potential of -0.7 MPa (day 19). Twenty days after the establishment of drought stress, growth variables, photosynthetic parameters, water potential, and leaf water loss were evaluated. Leaf, stem, and root sections were collected for anatomical analyses. Leaf samples were collected in three time points: “end of dark" (6:00 am), “mid-light", and end of the light period (6:00 pm), and immediately frozen in liquid nitrogen and stored at -80 °C for subsequent biochemical and molecular analyses.

Plant Water Status

Plant water status was determined throughout the experiment using a Scholander-type pressure chamber (Model 1000; PMS Instruments, Albany, NY, USA) at early morning (am) and midday (md). The first pair of leaves, fully expanded from the apex to the base, was cut at petiole insertion and immediately placed in the chamber to measure water potential (Ψw) (Scholander et al. 1964). The results are expressed in MPa.

To determine water loss, the leaves were detached, kept on plates with the abaxial side facing up, and their weight was measured on a precision analytical balance at 15-min intervals over a 4-h period. Water loss was calculated as the percentage of fresh weight loss relative to the initial fresh weight (Araújo et al. 2011a).

Growth Analysis

The stem length, largest root length, total dry weight, leaf number, and leaf area were measured 20 days after the establishment of drought stress. To determine leaf area, the leaves were detached and fixed individually on white plasticized graph paper. Photographs were taken with a digital camera and processed using ImageJ software (Schneider et al. 2012). Dry weight was obtained by oven-drying the plant material at 50 °C for 72 h.

Gas Exchange Parameters

The second pair of leaves, fully expanded from the apex to the base, A_N, *gs*, *E*, C_i, and instantaneous WUE (calculated as A_N/E) were evaluated using an infrared gas analyzer (LI-6400; Li-Cor Inc., Lincoln, Ne, USA) following 1 h of illumination during the light period under PPFD of 1000 µmol m^{-2} s^{-1}. The reference [CO_2] was 400 mol mol^{-1} air in plants under a[CO_2] and 800 µmol mol^{-1} air in plants under e[CO_2]. All measurements were performed using a 2-cm^2 leaf chamber at 25 °C, and a leaf-to-air vapor pressure deficit of 1.2–2.0 kPa. Blue light was set to 10% PPFD to optimize the stomatal aperture.

Metabolite Analysis

Leaf samples, consisting of the second fully expanded leaf from the apex, were harvested at the same time points described above. The samples were flash-frozen in liquid nitrogen, ground, and lyophilized for further analysis. Approximately 10 mg of lyophilized tissue was extracted with methanol, as described by Lisec et al. (2006). Photosynthetic pigments were determined as described by Porra et al. (1989) and anthocyanin by Neff and Chory (1998). Carbohydrates (starch, sucrose, glucose, and fructose) were evaluated, as described by Fernie et al. (2001). Protein and total amino acid levels were analyzed as described by Gibon et al. (2004). Malate content was determined as described by Nunes-Nesi et al. (2007). Proline content was determined following the methodology proposed by Bates et al. (1973), with modifications, as described previously by Felipe et al. (2019b). The results of the photosynthetic pigments were expressed in µg mg^{-1} of dry weight (DW); carbohydrates and amino acids in µmol mg^{-1} DW; proteins in mg g^{-1} DW; proline in µmol g^{-1} DW; and malate in nmol mg^{-1} DW.

Other metabolites of interest were quantified by gas chromatography-mass spectrometry (GC–MS). Approximately 10 mg of lyophilized leaf tissue, harvested in the middle of the light period, was homogenized in 1.5 mL of extraction solution (water:methanol:chloroform, 1:2.5:1 v/v), as previously described by Fiehn (2007), using 5 µM ribitol (Sigma-Aldrich) as internal standard. Of the soluble extract, 30 µL were subjected to vacuum drying and subsequent derivatization in two steps using an MPS dual-head autosampler (Gerstel, Mülheim an der Ruhr, Germany), as described by Gu et al. (2012). Following a 2 h incubation period at room temperature, the samples were analyzed as previously described (Shim et al. 2020) using a 7200 GC-QTOF system (Agilent Technologies, Santa Clara, CA, USA). Peaks were integrated using MassHunter Quantitative vb08.00 software (Agilent Technologies). For relative quantification, metabolite peak areas were normalized to the corresponding dry weight and peak area of ribitol.

Enzyme Analysis and Lipid Peroxidation

Activities of catalase (CAT; EC 1.11.1.6), ascorbate peroxidase (APX; EC 1.11.1.11), superoxide dismutase (SOD; EC 1.15.1.1), and peroxide oxidoreductase (POD; EC1.11.1.7) were quantified. Briefly, 50 mg of leaf samples were collected at the middle of the light period, snap frozen, homogeneized in liquid N and proteins were extracted in 1 mL extraction medium containing 0.1 M potassium phosphate buffer (pH 6.8) 0.1 mM ethylenediaminetetraacetic acid, 1 mM phenylmethylsulfonyl fluoride, and 1% (w/v) polyvinylpolypyrrolidone. In accordance with the recommended procedure (Nakano and Asada 1981), ascorbate was added to the extraction buffer prior to the APX extraction. Subsequently, the samples were centrifuged at 16,000 g for 15 min at 4 °C, and the supernatant was removed and set aside on ice for enzymatic assays plus protein determination (Bradford 1976). CAT, APX, and POD activities were determined as described previously (Chance and Maehly 1955; Nakano and Asada 1981; Havir and McHale 1987) and expressed as μmol^{-1} min^{-1} mg^{-1} protein. SOD activity was measured as previously described (Giannopolitis and Ries 1977) and expressed as U min^{-1} mg^{-1} protein, with 1 U being equivalent to the concentration of SOD required to inhibit 50% of nitro blue tetrazolium photoreduction.

Lipid peroxidation was determined by quantifying malondialdehyde (MDA), as proposed by Lima et al. (2002), with some modifications. The extraction was performed by adding 1 mL of 1% trichloroacetic acid (TCA) to 50 mg of fresh or macerated leaf samples. The solution was vortexed and centrifuged at 12,000 *g* for 15 min and 4 °C, after which 125 µL of the supernatant was transferred to new tubes, along with 375 µL of 0.5% 2-thiobarbituric acid (w/v) in 20% TCA (w/v). The reaction proceeded for 30 min with shaking at 95 °C and was blocked by incubation in an ice bath. The supernatants were transferred to new tubes, centrifuged at 10,000 *g* for 10 min and 4 °C, and read on a spectrophotometer at 532 and 600 nm. The means of the triplicates were obtained from absorbance values, and the MDA concentration was determined using the equation of Heath and Packer (1968). The results were expressed in nmol g^{-1} dry weight.

Quantification of 20E

20E was quantified as described by Corrêa et al. (2015). Methanolic extracts from leaf, stem, and root samples collected after 21 days of drought stress were prepared in 15-mL Falcon tubes with 100 mg of powdered dried plant material in 10 mL of methanol, and they were incubated at room

temperature under agitation for 7 days. The extracts were then centrifuged at 5,000 rpm for 20 min in 15-mL Falcon tubes, and the supernatant was transferred to 1.5-mL Eppendorf tubes and centrifuged again under the same conditions. After the second centrifugation, the supernatant was transferred to 1.5-mL vials. 20E was assayed on a Proeminence liquid chromatography system (Shimadzu, Kyoto, Japan) equipped with a reverse-phase column (150 mm × 4.6 mm, 5-µm particle size; C18 stationary phase) from Phenomenex (Torrance, CA, USA) and a Shimadzu SPD-M20A photodiode array detector at 246 nm. The mobile phase was 1:1 (v/v) methanol:water, with a flow rate of 1.0 mL min^{-1}, injection volume of 20 µL, and reading at 245 nm for 15 min. A 20E standard solution (Sigma-Aldrich) was prepared to construct the calibration curve (0–120 mg L^{-1}). 20E content was expressed as mg g^{-1} dry weight, while 20E production was expressed in g $plant^{-1}$.

Anatomical Characterization

Transverse sections of the midrib of leaves at three phenological stages (expanding, mature, and senescent) and stems from the midrib of the fourth internode were used. The samples were fixed in Karnovsky's solution (Karnovsky 1964), and kept refrigerated. After fixation, the samples were dehydrated in an ethanolic series and placed in acrylic resin (Historesin; Leica Instruments, Wetzlar, Germany). Transverse Sects. (5 µm in thickness) were obtained using an automated rotary microtome (RM2155; Leica Microsystems Inc., Buffalo Grove, IL, USA). For structural characterization, the samples were stained with toluidine blue (pH 3.2) for 3 min (O'Brien and McCully 1981). Sections were mounted on glass slides using synthetic Permount® SP15-500 resin (Thermo Fisher Scientific, Waltham, MA, USA) and observed under a light microscope. Images were captured using a light microscope (AX70 TRF; Olympus Optical, Tokyo, Japan) with a U-photo system coupled to a digital color camera (Spot Insight 3.2.0; Diagnostic Instruments Inc., Sterling Heights, MI, USA) and a microcomputer with the Spot Basic image capture program.

RNA Extraction, cDNA Synthesis, and Quantitative Real-Time PCR Analysis

Total RNA was extracted from shoot samples using TRI Reagent® (Sigma-Aldrich) according to the manufacturer's instructions. RNA was treated with DNase I (Thermo Scientific NanoDrop Technology, Wilmington, DE, USA) to remove genomic DNA contamination. cDNA was synthesized using the Super Script™ III kit (Invitrogen, Carlsbad, CA, USA). The expression of *P. glomerata* genes belonging to the lignin biosynthesis pathway, including cinnamate 4-hydroxylase (*PgC4H*), caffeoyl-CoA O-methyltransferase (*PgCCoAOMT*), cinnamoyl-CoA reductase (*PgCCR*), and cinnamyl alcohol dehydrogenase (*PgCAD*), was evaluated (Batista et al. 2019a). The *glyceraldehyde-3-phosphate dehydrogenase* (*GAPDH*) gene was used for normalization (Batista et al. 2019b). Real-time PCR was performed on a CFX96 Touch™ device (Bio-Rad Technologies, Hercules, CA, USA) using the SYBR Green Master Mix (Bio-Rad Technologies). The reactions included three biological replicates, each with duplicates. The reaction volume was 10 µL and included 4 µL SYBR-Green, 0.2 µL of each primer, 3.6 µL diethylpyrocarbonate-treated water, and 2 µL (10 ng μL^{-1}) cDNA. Amplification conditions were as follows: 2 min at 50 °C and 10 min at 95 °C, followed by 40 cycles at 95 °C for 15 s and 60 °C for 60 s, and a dissociation curve from 60 to 95 °C at 0.5 °C s^{-1}. Transcript levels were determined using the $2^{-\Delta\Delta Ct}$ method (Livak and Schmittgen 2001) with three biological replicates and at least two technical replicates each.

Proteomic Analysis

Comparative proteomic analyses were performed using freeze-dried and homogenized leaf samples (three biological replicates). Total protein extraction, digestion, and mass spectrometry analysis were performed as described by Oliveira et al. (2022). Spectra processing and database searching were performed using ProteinLynx Global Server software v. 3.0.2 (Waters, Milford, MA, USA), as described by Reis et al. (2021). The *P. glomerata* protein sequence database (Batista et al. 2019a) was used for protein identification. Comparative label-free quantification analysis was performed using ISOQuant software v. 1.7 (Distler et al. 2014). Raw mass spectrometry proteomic data were deposited in the ProteomeXchange Consortium via the PRIDE (Perez-Riverol et al. 2022) partner repository under accession number PXD040626. To ensure the quality of the results after data processing, only proteins present in all three biological replicates or absent from them (for unique proteins) were considered in differential accumulation analysis using Student's *t*-test ($P < 0.05$). Log_2 FC was used to identify differentially accumulated proteins (DAPs): they were considered upregulated when Log2 FC > 0.6 and downregulated when Log_2 FC < -0.6. DAPs were described and functionally annotated using the OmicsBox software (https://www.biobam.com/omicsbox). Protein sequences were subjected to a BLAST search against the National Center for Biotechnology Information non-redundant green plant protein database (taxon: 33,090, Viridiplantae). Enrichment of biological processes and cellular components in DAPs was analyzed by Fisher's exact test ($P < 0.01$) using OmicsBox. Kyoto Encyclopedia of Genes and Genomes (KEGG)

enrichment pathway analysis of DAPs ($P<0.01$) was performed. A protein–protein interaction network was constructed using orthologs identified by STRING (Szklarczyk et al. 2021) and the *P. glomerata* amino acid sequence.

Statistical Analysis

Statistically significant differences were determined by analysis of variance (ANOVA; F test) using the Genes software (Cruz 2016). Positive and negative correlation coefficients (R) among the variables were classified as no (0.0–0.2), weak (0.2–0.4), moderate (0.4–0.6), strong (0.6–0.8), or very strong (0.8–1.0). Proteomic analysis employed a Student's *t*-test ($P\leq0.05$) to assess statistical significance. Differentially accumulated proteins (DAPs) were determined using Log2 fold change (FC), considering proteins as upregulated when Log2 FC > 0.6 and downregulated when Log2 FC < -0.6.

Results

Elevated CO_2 Delays the Decrease in Water Potential Under Drought Conditions

Plants of *P. glomerata* were grown under a[CO_2] or e[CO_2], and well-watered (WW) or drought-stressed (D) conditions (Fig. 1a). Most analyzed parameters were affected by [CO_2], by watering regime, or by the interaction between these two factors (Table S1). The water status of the plants was determined in the morning (Ψ_{am}) and at midday (Ψ_{md}) for 20 days (Fig. 1b-e), until the plants in the a[CO_2] D treatment reached Ψ_{md} = -0.7 MPa (Fig. 1c). Both Ψ_{am} and Ψ_{md} were lower (± 1.5–fourfold) in drought-stressed plants than in well-watered individuals, regardless of [CO_2] (Fig. 1b–e). After 20 days of stress, a[CO_2]D plants reached Ψ_{am} = -0.46 MPa (Fig. 1d) and Ψ_{md} = -0.73 MPa (Fig. 1e). In contrast, e[CO_2]D plants maintained 25% less negative values, with Ψ_{am} = -0.35 MPa (Fig. 1d) and Ψ_{md} = -0.53 Mpa (Fig. 1e).

Measurements of water loss in detached leaves showed that, within the first 15 min, drought-stressed plants grown under ambient CO_2 (a[CO_2]D) had significantly lower water loss than well-watered controls. In e[CO_2]D plants, however, this difference did not appear until 45 min (Fig. 1f). Leaf water loss in drought-stressed plants remained consistently below that of their well-watered counterparts after 4 h of analysis: 12% for a[CO_2]D and 20% for e[CO_2]D (Fig. 1f). Pearson's correlation analyses revealed a strong negative correlation (R = -0.9; P = 0.00000351) between plant water potential and leaf water loss (Fig. 1g). Pearson's correlation analysis revealed a strong negative correlation (R = −0.9; P = 0.00000351) between plant water potential and leaf water loss (Fig. 1g), indicating that plants with more negative Ψ values were associated with lower rates of leaf water loss.

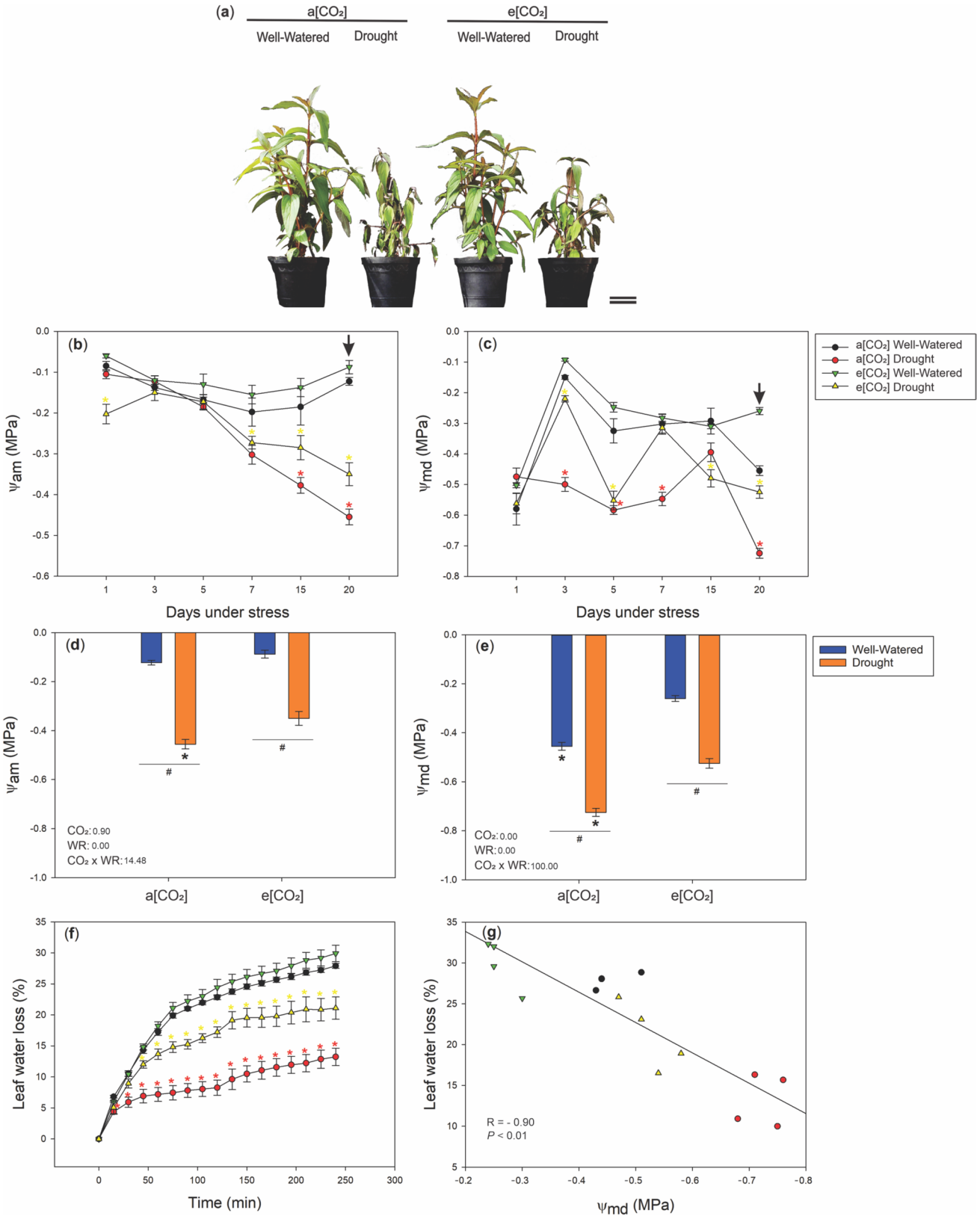
Fig. 1 Phenotype and water potential in 41-day-old *Pfaffia glomerata* plants (accession 22), under ambient (a[CO_2]) and elevated CO_2 concentration (e[CO_2]) and 20 consecutive days of well-watered and drought-stressed conditions. (**a**) Appearance of the plants, Bar = 10 cm. (**b**) water potential measured in the morning (Ψam) and (**c**) at midday (Ψmd) during the period of stress. (**d**) Water potential in the morning and (**e**) at midday after 20 days of stress. (**f**) Leaf water loss and (**g**) linear correlation between Ψmd vs. leaf water loss. The arrows in panels **b** and **c** indicate the day gas exchange analyses were performed and samples were collected. Asterisks in panels **b**, **c**, and **f** indicate significant differences by F test ($P\leq0.05$) among watering regimes compared to the same CO_2 treatments. In panels **d** and **e**, asterisks (*) indicate differences between CO_2 treatments within the same watering regime; hashtags (#) indicate differences between watering regimes within the same CO_2 supply by F test ($P\leq0.05$). In panel **g**, points represent the average of replicas and coefficient of correlation (R); the p-value (*p*) is shown in the figure. Data represent the mean of four biological replicates ($n=4$) ± standard error. The ANOVA results showed a significant interaction between the factors ([CO_2] x watering regimes (WR)) for most variables; for details see Table S1

Elevated CO_2 Modulates Water Use Efficiency (WUE) Under Drought Conditions

Drought stress elicited marked changes in gas exchange parameters (Fig. 2). Significant interactions between CO_2 concentration and watering regime were detected for stomatal conductance (*gs*), transpiration rate (*E*), intercellular CO_2 concentration (*C*i), and WUE ($P<0.05$; Table S1). Drought caused substantial reductions in net CO_2 assimilation—A_N (78% and 73%), *gs* (91% and 92%), and *E* (86% and 92%) in plants grown under ambient and elevated CO_2, respectively, relative to well-watered controls (Fig. 2a–c). Although A_N and *E* showed comparable absolute values in drought-stressed plants grown under ambient and elevated CO_2, plants under elevated CO_2 exhibited lower *gs* (Fig. 2b) and higher *C*i (Fig. 2d). Consequently, instantaneous water use efficiency (WUE = A_N /*E*) increased by 195% under elevated CO_2 and drought (Fig. 2e). No significant differences in WUE were observed under ambient CO_2 between irrigation regimes.

Drought Stress and e[CO_2] Affect Growth

After 20 days of exposure to drought conditions, the growth of *P. glomerata* was drastically affected (Fig. S2). Significant interactions were observed between the factors ([CO_2] × watering regime) for the largest root length, total dry weight, and stem and root biomass partitioning, and the results differed significantly ($p<0.05$) for these variables (Table S1). Compared with well-watered plants, plants


(a)
a[CO2]
e[CO2]
Well-Watered
Drought
Well-Watered
Drought
(b)
ψam (MPa)
Days under stress
(c)
ψmd (MPa)
Days under stress
a[CO2] Well-Watered
a[CO2] Drought
e[CO2] Well-Watered
e[CO2] Drought
(d)
ψam (MPa)
CO2: 0.90
WR: 0.00
CO2 x WR: 14.48
a[CO2]
e[CO2]
(e)
ψmd (MPa)
CO2: 0.00
WR: 0.00
CO2 x WR: 100.00
a[CO2]
e[CO2]
Well-Watered
Drought
(f)
Leaf water loss (%)
Time (min)
(g)
Leaf water loss (%)
R = - 0.90
P < 0.01
ψmd (MPa)

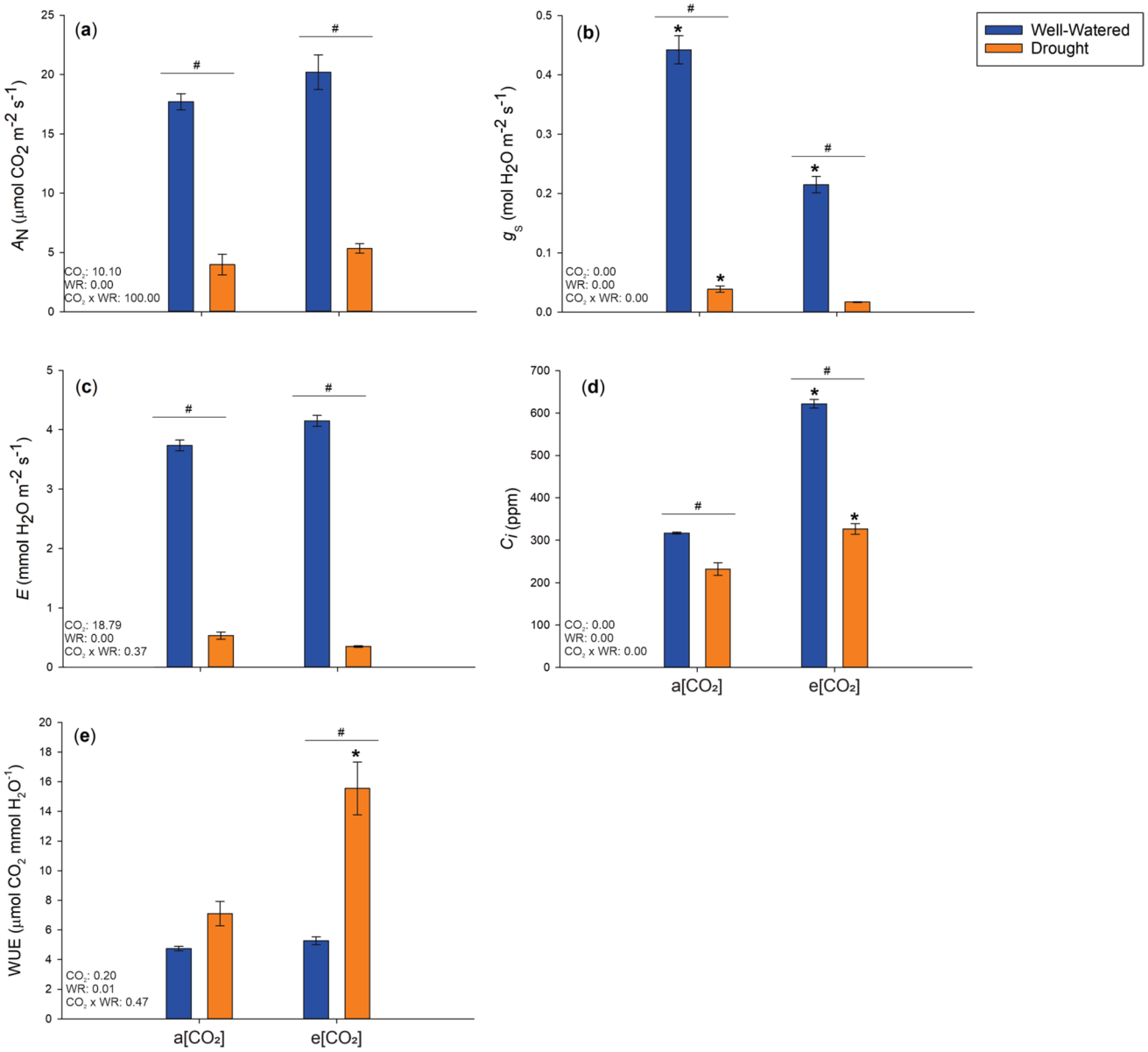


Fig. 2 Gas exchange parameter in 41-day-old *Pfaffia glomerata* plants (accession 22), under ambient (a[CO_2]) and elevated CO_2 concentration (e[CO_2]) and 20 consecutive days of well-watered and drought-stressed conditions. (**a**) Net CO_2 net assimilation rate (A_N). (**b**) Stomatal conductance (g_s). (**c**) Transpiration rate (E). (**d**) Internal CO_2 concentration (C_i). (**e**) Instantaneous water use efficiency (WUE). Asterisks (*) indicate differences between CO_2 treatments within the same watering regime; hashtags (#) indicate differences between watering regimes within the same CO_2 supply by F test ($P \leq 0.05$). Data represent the mean of six biological replicates ($n = 6$) ± standard error. The ANOVA results showed a significant interaction between the factors ([CO_2] x watering regimes (WR)) for most variables; for details see Table S1

grown under a[CO_2]D and e[CO_2]D showed a reduction in leaf area (71% and 66%), number of leaves (26% and 36%), stem length (24% and 35%), largest root length (29% and 14%), respectively and reduction in total dry weight (38%) under a[CO_2]D (Fig. S2a-e). Under drought conditions, a[CO_2]D favored increased the root/shoot ratio (131%) and biomass accumulation in the roots (70%), but promoted reduction the biomass accumulation in the stem (32%); whereas e[CO_2]D did not altered biomass accumulation in the stem and root and root/shoot ratio (Fig. S2f-g), compared to the well-watered controls. Conversely, biomass partitioning in the leaves did not differ between drought conditions (Fig. S2g). A comparison of drought-stressed and irrigated controls, revealed approximately 20% reduction in leaf biomass partitioning at both [CO_2] (Fig. S2g).

Primary Metabolism Changes in Response to [CO_2] and Drought Stress

Primary metabolism was influenced by [CO_2] and drought stress (Table 1**,** Fig. S3 and Fig. S4). For most of the metabolites analyzed, interactions between the factors ([CO_2] × watering regime) were verified, except for starch and free amino acids ("end of dark period" and "end of light period"), protein ("mid-light period" and "end of light period"), glycerate, threonate, malate, and proline, and the results differed significantly ($p < 0.05$) (Table S1). As shown in Fig. S3, e[CO_2]D decreased the photosynthetic pigment content in plants under drought conditions. In particular, a significant reduction was observed for Chl *a* (26%), Chl *b* (35%), total Chl (25%), the Chl *a*/Chl *b* ratio (7%) (Fig. S3a–d), and carotenoids (24%) (Fig. S3e) compared to well-watered plants. In contrast, a[CO_2]D did not alter chlorophyll and carotenoid levels (Fig. S3a–e), relative to well-watered controls. Similarly, anthocyanin levels did not differ across treatments (Fig. S3f).

We further analyzed the content of primary metabolites and the relative content of nine metabolites by GC–MS in the samples collected at the "mid-light period" timepoint (Table 1). We also analyzed the content of soluble sugars, starch, total free amino acids and protein at dawn and dusk. The levels of these metabolites did not show a specific diurnal pattern (Table 1 and **S4**). In the samples collected at the middle of the light period, plants grown under e[CO_2]D conditions showed increased levels of osmolytes, including glucose (360%), fructose (275%), and myo-inositol (47%) (Table 1), compared to their irrigated controls. In addition, plants exposed to e[CO_2]D we observed an increased glutamate (282%), serine (184%), and valine (177%); but contained less alanine (66%), aspartate (73%), glycerate (40%), and threonate (30%) (Table 1). Under drought conditions, there was no change in the levels of sucrose, starch, malate, glycine, proline, free amino acids and protein content (Table 1) compared to well-watered controls. In contrast, plants grown under a[CO_2]D condition showed little difference in the levels of these metabolites. We observed decreased threonate (20%) and glycine (63%) (Table 1), whereas the other metabolites did not differ from those in well-watered controls.

Drought and e[CO_2] Alter Antioxidant Enzyme Activity

We then measured the activities of antioxidant enzymes, including APX, CAT, SOD, and POD, and found that this antioxidant system was differentially affected by watering regime and [CO_2] (Fig. 3). ANOVA clearly indicated significant interactions between these factors for these variables ($p < 0.05$) (Table S1). Furthermore, plants exposed to a[CO_2]D showed increased CAT (117%) and SOD (57%) activity and MDA levels (90%) (Fig. 3b and e). Still, they decreased POD (32%) activity compared to their well-watered controls (Fig. 3c). In plants grown under e[CO_2]D increases in APX (58%), CAT (135%) (Fig. 3a-b), SOD (35%) (Fig. 4d) activities and MDA levels (76%) were observed, relative to their well-watered counterparts. No difference in APX was observed in plants exposed to a[CO_2]D, or for POD in plants under e[CO_2]D condition (Fig. 3a and c) relative to their well-watered counterparts.

Anatomical Changes Induced by Drought Conditions

No remarkable structural changes were observed in the leaf anatomy of plants exposed to different [CO_2] and irrigation conditions (Fig. S5a–h). The leaves consisted of a uniseriate epidermis, a large central vascular bundle with parenchyma distributed along the main vein, a subepidermal collenchyma on the adaxial side, and a lamina subdivided into palisade and lacunar parenchyma (Fig. S5a–h). Instead, drought promoted changes in stem and root anatomy (Fig. S5i–x). In general, the stems exhibited uniseriate epidermis, subepidermal collenchyma, a fiber thread above the vascular system, and thickened cell walls in the interfascicular region, thereby forming a continuous ring (Fig. S5i–p). Secondary growth was accounted for by the vascular cambium, which mainly produced xylem (Fig. S5i–p). In addition, plants grown under a[CO_2]D condition exhibited more differentiated vascular tissue, with stronger vascular cambium activity and pronounced secondary xylem formation (Fig. S5k, l). Overall, cross-sections of the roots showed an irregularly shaped uniseriate epidermis, a cortex with rounded and juxtaposed cells, and a well-developed vascular cambium, with a predominance of vessel elements (Fig. S5q–x). Regardless of [CO_2], drought promoted the density of vessel elements in the central vascular root bundle (Fig. S5s, t, w, x).

Drought Promotes the Expression of Lignin Synthesis Genes

The expressions of *P. glomerata* genes belonging to the lignin biosynthesis pathway, including cinnamate 4-hydroxylase (*PgC4H*), caffeoyl-CoA O-methyltransferase (*PgCCoAOMT*), cinnamoyl-CoA reductase (*PgCCR*), and cinnamyl alcohol dehydrogenase (*PgCAD*) were influenced by drought and [CO_2]. ANOVA showed interactions between the factors ([CO_2] × watering regime) for all genes analyzed, and the results differed ($p < 0.05$) for these genes (Table S1). We observed that e[CO_2]D induced the expression of lignin biosynthesis-related genes in response to drought (Fig. 4).

Table 1 Content of metabolites and relative response value (RRV) from GC–MS at "mid-light period" involved in carbon metabolism in 41-day-old *Pfaffia glomerata* plants (accession 22), under ambient ($a[CO_2]$) and elevated CO_2 concentration ($e[CO_2]$) and 20 consecutive days of well-watered and drought-stressed conditions. GC–MS data were normalized to the corresponding dry weight and peak area of the internal standard (ribitol)

Variables	$a[CO_2]$WW	$a[CO_2]$D	$e[CO_2]$WW	$e[CO_2]$D
Carbohydrates				
Glucose (µmol mg^{-1} DW)	0.03 (±0.004)*	0.02 (±0.002)	0.01 (±0.002)	0.06 (±0.006)*#
Fructose (µmol mg^{-1} DW)	0.02 (±0.008)	0.02 (±0.003)	0.02 (±0.004)	0.08 (±0.009)*#
Sucrose (µmol mg^{-1} DW)	0.05 (±0.003)	0.04 (±0.001)	0.04 (±0.0009)	0.05 (±0.003)
Starch (µmol mg^{-1} DW)	0.10 (±0.004)	0.06 (±0.011)	0.12 (±0.003)	0.14 (±0.011)*
Myoinositol (RRV)	257.56 (±3.27)	281.71 (±13.18)	298.72 (±12.73)	439.02 (±19.35) *#
Amino acids				
α-Alanine (RRV)	59.05 (±5.28)	52.77 (±6.91)	92.33 (±7.75)#	31.16 (±3.72)
Aspartate (RRV)	10.88 (±1.76)	8.51 (±0.60)	27.97 (±3.33)*#	7.55 (±1.63)
Glycine (RRV)	69.07 (±7.36)#	25.87 (±1.99)	43.29 (±1.58)	42.93 (±3.38)
Glutamate (RRV)	16.61 (±2.15)	19.10 (±3.20)	18.47 (±2.42)	70.64 (±7.19)*#
Proline (µmol g^{-1} DW)	1.61 (±0.12)*	1.64 (±0.07)*	1.10 (±0.11)	0.97 (±0.03)
Serine (RRV)	31.73 (±0.58)	47.80 (±8.98)	23.86 (±2.22)	67.69 (±4.50)#
Valine (RRV)	20.39 (±1.99)	27.62 (±3.24)	14.69 (±0.95)	40.62 (±2.21)#
Amino acid (µmol mg^{-1} DW)	114.80 (±10.62)	71.93 (±6.64)	87.50 (±13.91)	138.92 (±7.64)
Organic acids				
Glycerate (RRV)	157.88 (±14.24)	137.08 (±6.10)	197.03 (±5.07) #	118.29 (±26.04)
Malate (nmol mg^{-1} DW)	4.76 (±0.58)	6.20 (±0.30)	5.35 (±0.23)	7.64 (±0.33)*
Threonate (RRV)	279.74 (±19.83)#	222.40 (±7.90)*	255.67 (±7.91) #	178.65 (±2.97)
Others				
Protein (mg g^{-1} DW)	28.30 (±0.64)	27.58 (±1.06)	31.04 (±1.90)	26.47 (±2.17)

Asterisks (*) indicate differences between CO_2 treatments within the same watering regime; hashtags (#) indicate differences between watering regimes within the same CO_2 supply by F test ($P \leq 0.05$). Data represent the mean of six biological replicates ($n = 4–6$) ± standard error. The ANOVA results showed significant interaction between the factors ($[CO_2]$ x watering regimes (WR)) for most variables; for details see Table S1.

Compared to the $a[CO_2]$WW control, $e[CO_2]$D showed upregulation of the *PgC4H* (fivefold), *PgCCR* (fourfold), and *PgCCoAOMT* (11-fold) genes (Fig. 4a–c). In comparison, $a[CO_2]$D affected positively the expression of *PgC4H* (twofold) and *PgCCoAOMT* (fourfold) (Fig. 4a, c), but negatively that of *PgCAD* (2.5-fold) (Fig. 4d).

Proteome Responses of the Leaves to Drought and High CO_2

Total leaf protein fractions were isolated from leaves harvested from plants after the drought stress and $e[CO_2]$ treatments and subjected to label-free proteomics. In total, 1040 proteins were identified, of which 921 (89%) were found in all four treatments (Fig. S6, Table S2). A total of 405 DAPs were identified (Fig. 5a, b). This analysis revealed significant changes in protein abundance in response to $e[CO_2]$ and water supply. Comparisons of $a[CO_2]$D/$a[CO_2]$WW, $e[CO_2]$D/$e[CO_2]$WW, $e[CO_2]$D/$a[CO_2]$D, and $e[CO_2]$WW/$a[CO_2]$WW revealed 96, 24, 10, and 17 accumulated proteins, respectively (Fig. 5a). Comparisons between $a[CO_2]$D/$a[CO_2]$WW, $e[CO_2]$D/e $[CO_2]$WW, $e[CO_2]$D/$a[CO_2]$D, and $e[CO_2]$WW/$a[CO_2]$WW revealed 68, 37, 4, and 1 downaccumulated proteins, respectively (Fig. 5b).

We grouped all proteins into functional categories using KEGG analysis to obtain an overview of the proteomic response to water stress and elevated CO_2. The identified DAPs were associated with 19 plant metabolic pathways (Fig. 5c, Table S3). Under ambient CO_2, the drought vs. well-watered comparison ($a[CO_2]$D/$a[CO_2]$WW) showed 18 upregulated and 18 downregulated pathways, with the largest groups corresponding to carbon metabolism (25 proteins), porphyrin metabolism (18), ribosomes (17), amino acid biosynthesis (16), cofactor biosynthesis (14), ascorbate and aldarate metabolism (11), and the TCA cycle (10). Under elevated CO_2, the drought vs. well-watered comparison ($e[CO_2]$D/$e[CO_2]$WW) revealed 14 upregulated and 13 downregulated pathways, particularly porphyrin metabolism (17), amino acid biosynthesis (13), and cofactor biosynthesis (12). Other contrasts displayed fewer differentially regulated pathways. In plants under drought, the comparison between elevated and ambient CO_2 ($e[CO_2]$ D/$a[CO_2]$D) yielded four upregulated and five downregulated pathways, including protein processing in the endoplasmic reticulum (4 proteins), amino acid biosynthesis (3), porphyrin metabolism (3), alanine–aspartate–glutamate metabolism (1), ascorbate and aldarate metabolism (1), cofactor biosynthesis (1), and carbon metabolism (1). Under well-watered conditions ($e[CO_2]$WW/$a[CO_2]$WW), 11 pathways were upregulated and five downregulated, mainly carbon metabolism (6 proteins), amino acid biosynthesis (3), cofactor biosynthesis (3), and porphyrin metabolism (3).

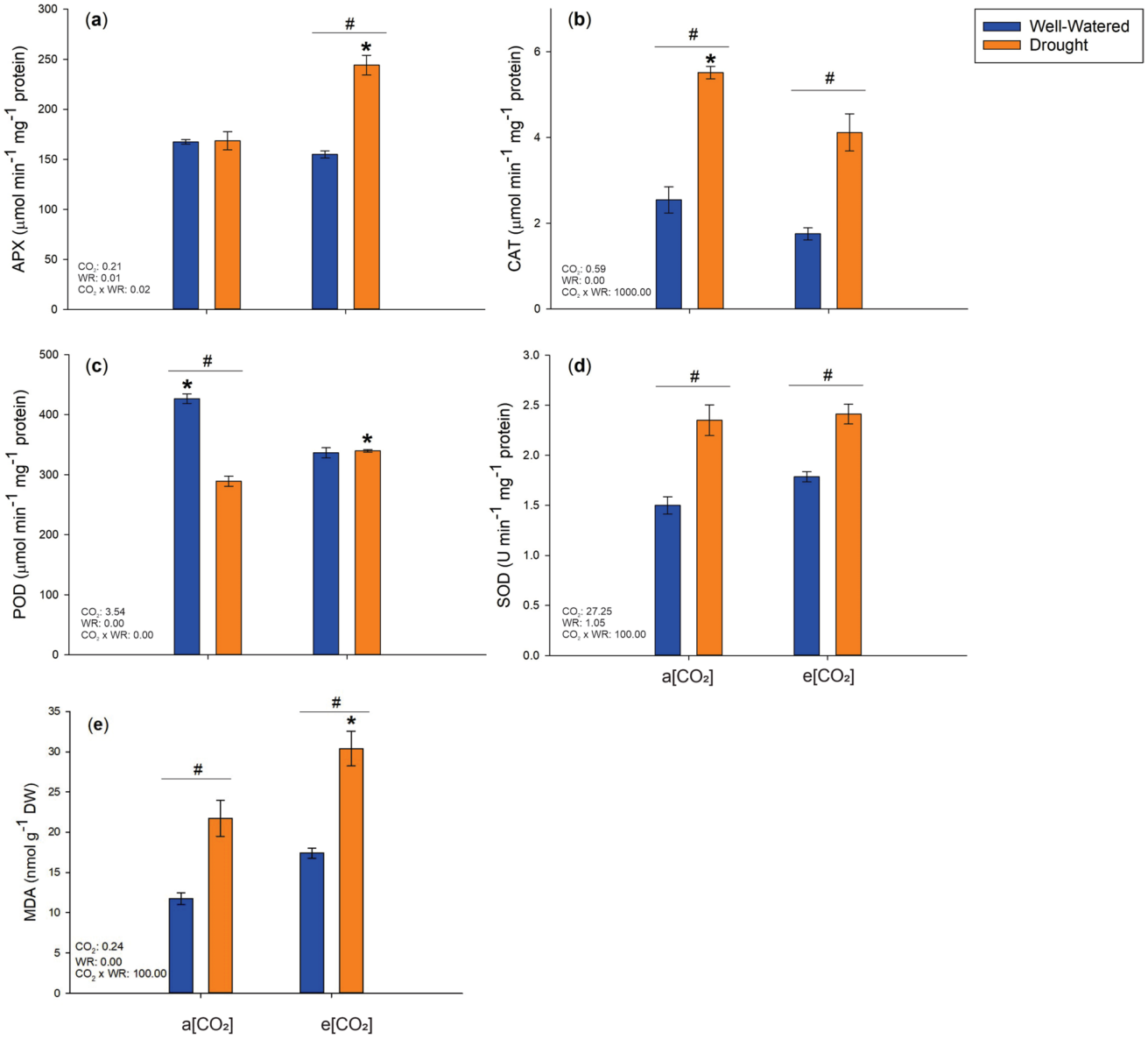


Fig. 3 Antioxidant enzymatic activity and lipid peroxidation (MDA content) in 41-day-old *Pfaffia glomerata* plants (accession 22), under ambient (a[CO_2]) and elevated CO_2 concentration (e[CO_2]) and 20 consecutive days of well-watered and drought-stressed conditions. (**a**) ascorbate peroxidase (APX); (**b**) Catalase (CAT); (**c**) peroxidases (POD); (**d**) superoxide dismutase (SOD) and; (**e**) malonaldehyde (MDA). Asterisks (*) indicate differences between CO_2 treatments within the same watering regime; hashtags (#) indicate differences between watering regimes within the same CO_2 supply by F test ($P \leq 0.05$). Data represent the mean of six biological replicates ($n = 6$) ± standard error. The ANOVA results showed a significant interaction between the factors ([CO_2] x watering regimes (WR)) for most variables; for details see Table S1

Gene Ontology (GO) analysis of DAPs was performed with OmicsBox and classified into biological processes, molecular functions, and cellular components (Fig. 6a, Table S4). Most upregulated proteins were associated with water-stress responses, including abiotic stimuli (32 proteins), oxidative stress (25), abscisic acid (22), oxidative detoxification (21), and water deprivation (20). Molecular functions were dominated by catalytic activity (310 proteins), transporter activity (60), and hydrolase activity (43). Upregulated DAPs were most abundant in mitochondria (148 proteins) and the cell wall (63 proteins), organelles central to oxidative stress responses and structural protection. As predicted, elevated CO_2 attenuated drought-responsive protein accumulation across most functional categories (Fig. 6a), except for two isoforms of a membrane steroid-binding 2-like protein involved in growth regulation, which remained more abundant under e[CO_2]D.

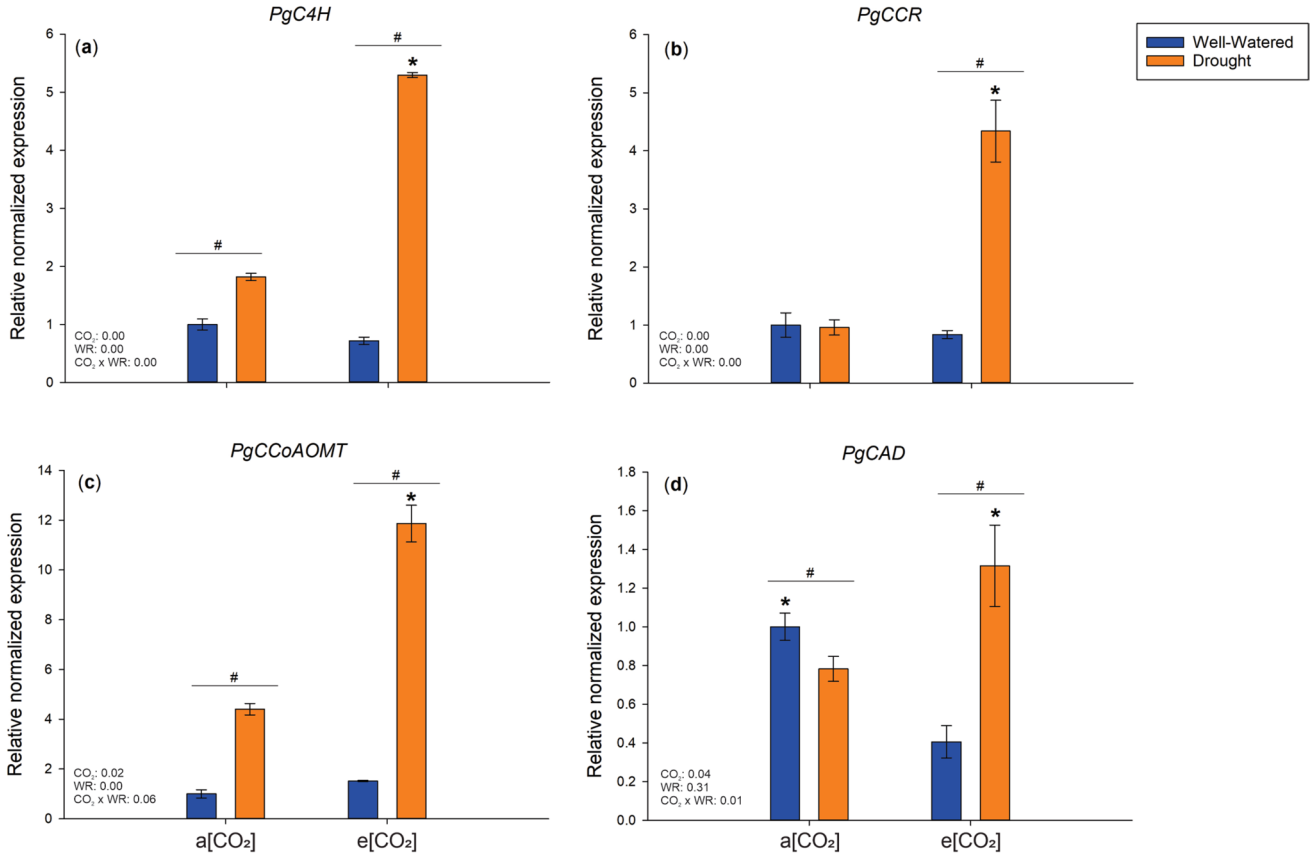


Fig. 4 Relative normalized expression of lignin biosynthesis genes in 41-day-old *Pfaffia glomerata* plants (accession 22), under ambient (a[CO_2]) and elevated CO_2 concentration (e[CO_2]) and 20 consecutive days of well-watered and drought-stressed conditions. (**a**) *PgC4H* gene; (**b**) *PgCCR* gene; (**c**) *PgCCoAOMT* gene; and (**d**) *PgCAD* gene. Gene expression is relative to the *glyceraldehyde-3-phosphate dehydrogenase* control gene. Asterisks (*) indicate differences between CO_2 treatments within the same watering regime; hashtags (#) indicate differences between watering regimes within the same CO_2 supply by F test ($P \leq 0.05$). Data represent the mean of three biological replicates ($n = 3$) ± standard error. The ANOVA results showed significant interaction between the factors ([CO_2] x watering regimes (WR)) for most variables; for details see Table S1

We further evaluated the predicted protein–protein interactions between the *Beta vulgaris* homologs. We observed that proteins from different pathways involved in the drought responded to a highly similar (Fig. 6b). To identify possible interactions between proteins related to 20E biosynthesis we performed a protein–protein interaction network analysis in isolation (Fig. 6c). Interestingly, the cytochrome P450 CYP72A219-like protein (cds.comp18142_c0_seq1), which was shown to be upregulated under e[CO_2]D condition in comparison with e[CO_2]WW condition (Table S2), interacted with five regulatory proteins of the sterol biosynthetic pathway: delta(14)-sterol reductase, delta(7)-sterol-C5(6)-desaturase, delta(7)-sterol-C5(6)-desaturase-like (2 isoforms), and 7-dehydrocholesterol reductase (Fig. 6c).

Elevated [CO_2] Associated with Drought has a Positive Effect on 20E Content

We assessed the combined effects of drought and [CO_2] on 20-hydroxyecdysone (20E) synthesis. ANOVA revealed significant interactions between [CO_2] and irrigation regime for whole-plant 20E content and production, except for 20E content in leaves and stems (Table S1). Overall, drought increased 20E content in leaves and stems under both [CO_2] conditions (Fig. 7a, c), whereas in roots the increase was significant only under e[CO_2] (Fig. 7e).

Under a[CO_2]D, 20E content increased in leaves (183%) and stems (33%), decreased in roots (20%), and showed no significant changes in 20E production in any organ compared with well-watered plants (Fig. 7b, d, f). Under e[CO_2]D, 20E content and production increased markedly in leaves (242% and 180%) and roots (115% and 123%), and 20E content increased in stems (89%) relative to the respective controls. These results indicate that drought enhances 20E

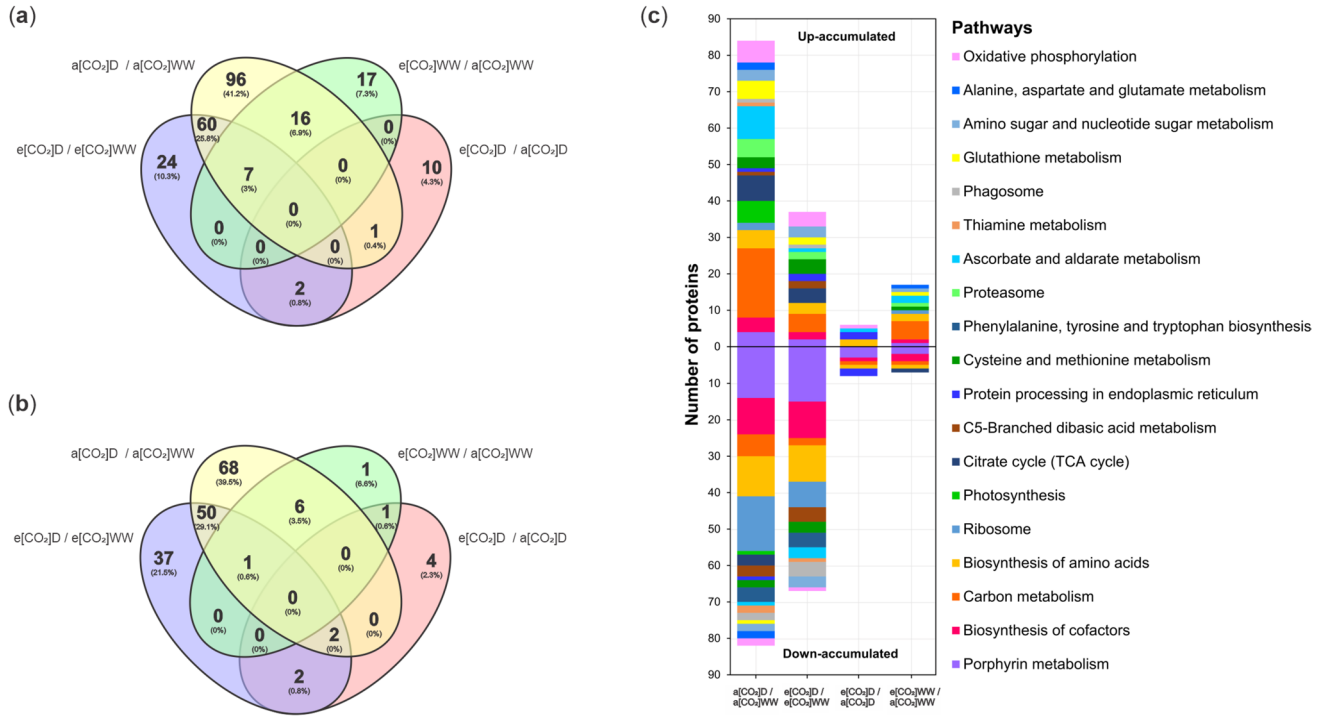


Fig. 5 Analysis of differentially accumulated proteins (DAPs) in 41-day-old *Pfaffia glomerata* plants (accession 22), under ambient ($a[CO_2]$) and elevated CO_2 concentration ($e[CO_2]$) and 20 consecutive days of well-watered and drought-stressed conditions. Venn diagram showing common (**a**) upregulated DAPs and (**b**) downregulated DAPs. (**c**) KEGG-based pathway enrichment analysis

synthesis regardless of [CO_2], although total plant 20E production is shaped by the interaction between water availability and atmospheric [CO_2].

Discussion

Relationship Between Drought, CO_2 and Metabolism (Metabolites and Proteome) and Possible Mechanisms of $e[CO_2]$ in Mitigating Drought Effects

Our findings indicate that elevated CO_2 does not uniformly affect plant traits but rather modulates drought responses in a context-dependent manner, with its influence becoming more apparent under water deficit conditions. Plants exposed to $e[CO_2]$D exhibited higher water potential and higher WUE (+195%), despite reduced stomatal conductance (g_s) (Qiao et al. 2010; Pazzagli et al. 2016; Ávila et al. 2020). In our dataset, CO_2 enrichment was particularly relevant for water relations under drought, as $e[CO_2]$D plants maintained less negative Ψ values than $a[CO_2]$D and displayed a marked increase in WUE, indicating that elevated CO_2 modulated the balance between carbon gain and water loss under stress within the chamber-level CO_2 environments imposed in this study, without compensating for drought-induced limitations.

Although WUE did not differ between irrigation regimes under ambient CO_2, elevated CO_2 increased WUE under drought, despite similar net CO_2 assimilation rates. This increase was associated with lower stomatal conductance and higher intercellular CO_2 concentration, indicating a stomatal rather than photosynthetic basis for WUE modulation. The WUE response at the leaf level is directly related to stomatal closure, which is essential to maintaining the integrity of the water transport system (Hatfield and Dold 2019; Birami et al. 2020). Importantly, the association between leaf water potential and leaf water loss reflects coordinated physiological regulation, primarily mediated by stomatal control, rather than a direct causal effect of Ψ on transpiration. Under drought stress, A_N is expected to decrease and may be accompanied by lower photosynthetic pigment content. Here, we noted that under $e[CO_2]$, drought-ed plants had lower pigment levels in leaves than well-watered plant, while under $a[CO_2]$, pigment levels remained unchanged between treatments (Fig. S3), indicating that the CO_2 level may influence the biosynthesis or degradation of these pigments (Li et al. 2019; Song et al. 2020). This pattern suggests that CO_2 enrichment reshaped photoprotective adjustments under drought, because pigment losses were detectable under $e[CO_2]$D but not under $a[CO_2]$D, even though drought reduced A_N at both CO_2 levels. Lower photosynthetic pigment content results in decreased light absorption, which in turn reduces the potentially damaging

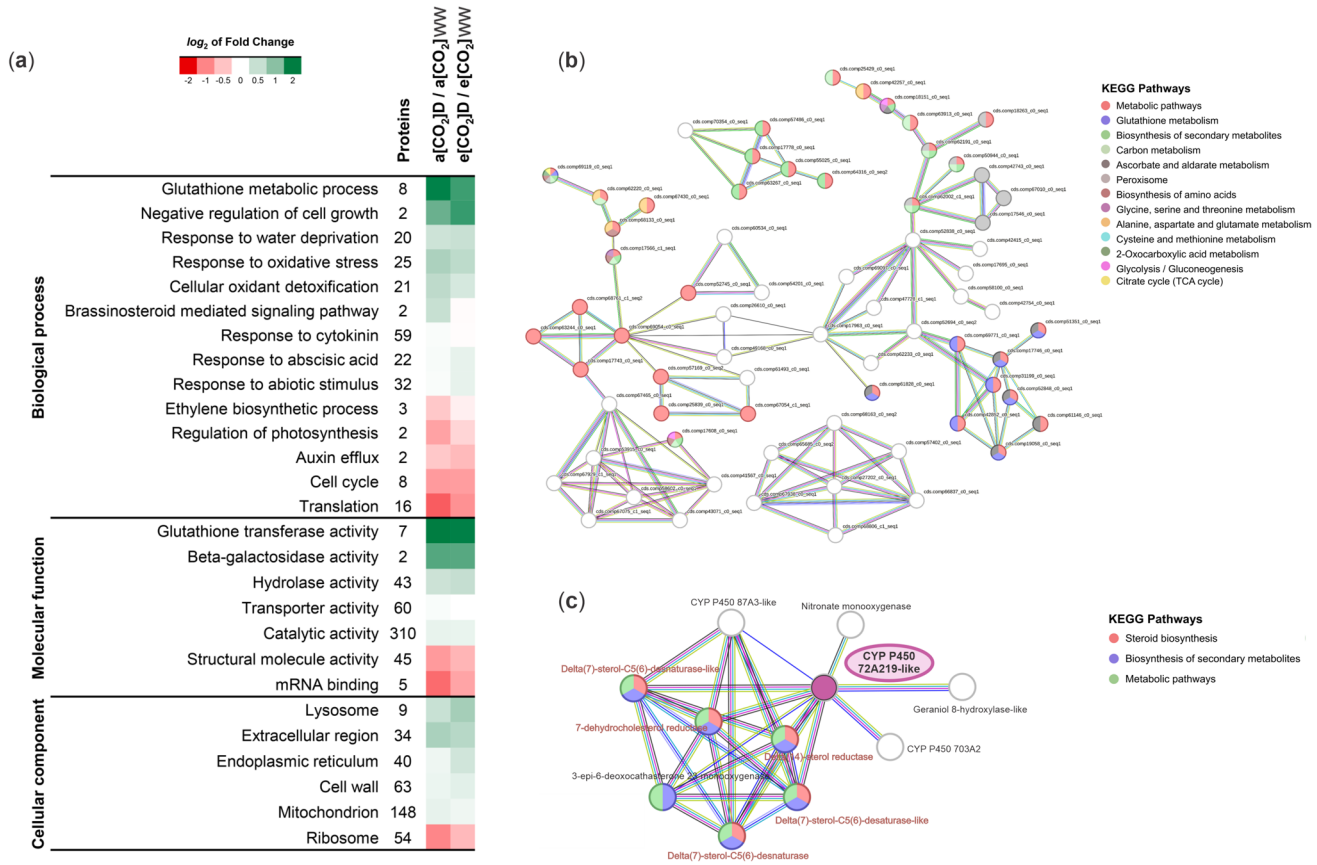


Fig. 6 Heatmap of differentially accumulated proteins (DAPs) and protein–protein interaction network between proteins with putative roles in 41-day-old *Pfaffia glomerata* plants (accession 22), under ambient (a[CO_2]) and elevated CO_2 concentration (e[CO_2]) and 20 consecutive days of well-watered and drought-stressed conditions. (**a**) Log_2 (FC) was used to calculate DAPs, with Log_2 FC > 0.6 indicating upregulated proteins and Log_2 FC < -0.6 downregulated proteins. Functional annotation related to DAPs is based on Gene Ontology (GO); downregulated proteins are denoted in red and upregulated in green. (**b**) The network view summarizes the network of predicted associations for a particular group of proteins from different pathways related to drought response. (**c**) Protein–protein interaction network between cytochrome P450 CYP72A219-like protein (purple). Note: The "node" circles represent proteins. Only first neighbors are shown in the interactions. The predicted interactions in the network had confidence > 0.9 in panels **b** and > 0.4 in panels **c,** according to the combined STRING score. The straight line shows the interaction between proteins. The lines represent the existence of the seven types of evidence used in predicting the associations: fusion (red line), neighborhood (green line), cooccurrence (blue line), experimental (purple line), textmining (yellow line), database (light blue line), and coexpression (black line)

warming effects of high solar radiation (Havaux and Tardy 1999). Furthermore, proteome analysis revealed that plants exposed to a[CO_2] and drought simultaneously invested in proteins of the photosynthetic machinery, such as photosystem subunits (Tables **S2, S3**), without an increase in A_N. Degradation of photosystem subunits may be associated with a high frequency of photo-oxidative damage (Batista-Silva et al. 2019). Notably, under e[CO_2]D, many stress-related proteins did not accumulate or were downregulated (Fig. 6a; Table S2), indicating that elevated CO_2 attenuated the canonical drought proteome signature at the chamber-environment scale, even though key physiological constraints on photosynthesis and growth remained evident. Collectively, these results suggest that the characteristic reduction in photosynthetic pigment levels and the non-investment in photosynthetic machinery in *P. glomerata* under e[CO_2]D reflect an acclimatory adjustment to drought stress rather than an effective adaptive or compensatory response, as drought-induced physiological constraints and growth penalties remained evident.

Despite the positive effects of lower g_s on water loss under drought stress, its reduction negatively affects A_n and, consequently, plant growth (Shinohara and Leskovar 2014). Drought alone reduced growth parameters, reflecting the severe stress imposed by total water limitation. Plants exposed to a[CO_2]D showed a higher root/shoot ratio. This may explain the increased number of vascular elements (xylem) and, consequently, the greater lignification in plants under drought conditions, as observed in this study. No root/shoot ratio increase was observed in plants previously exposed to e[CO_2]D. Therefore, our results suggest distinct morphophysiological response patterns associated

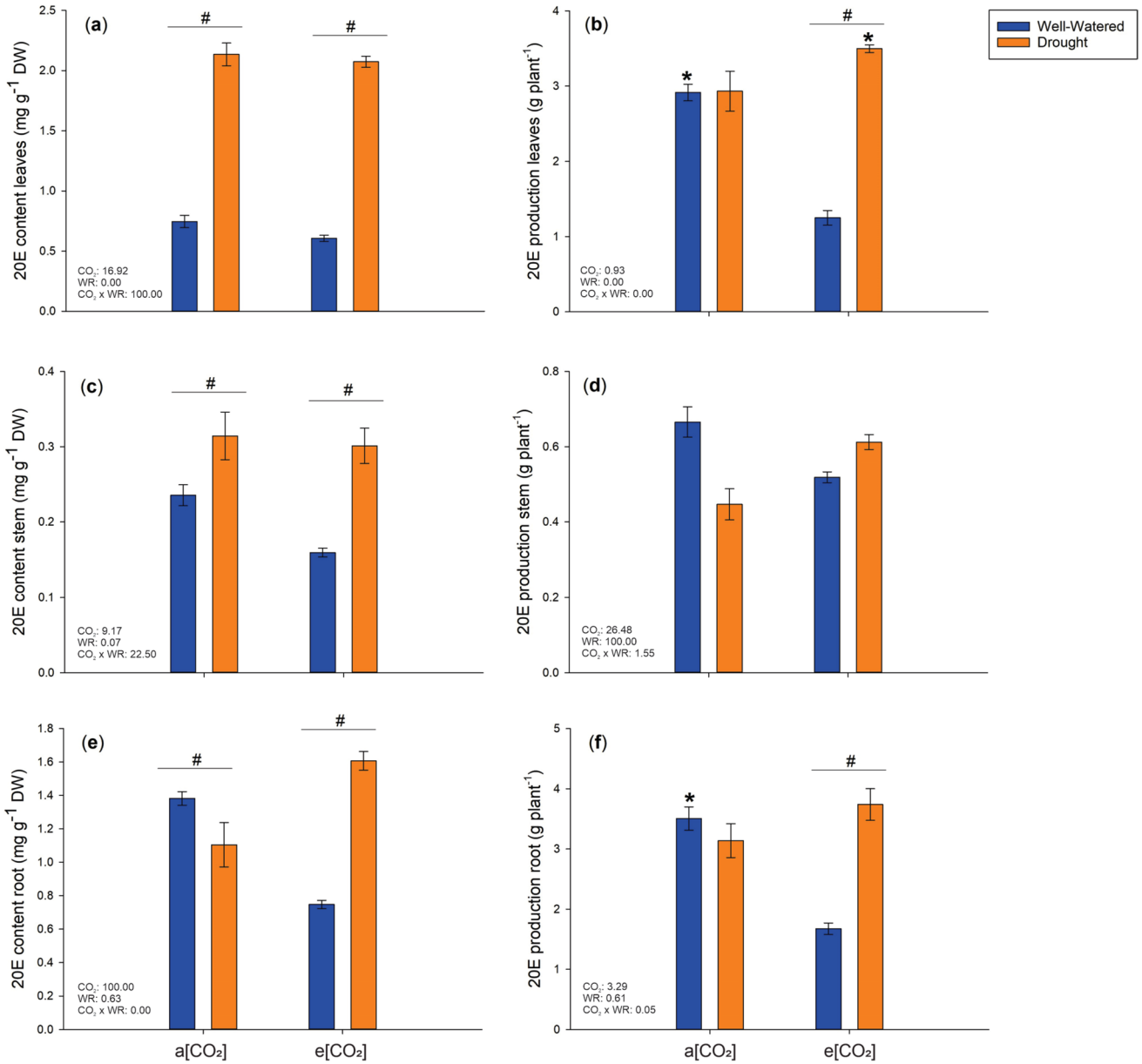


Fig. 7 20-hydroxyecdysone (20E) content in 41-day-old *Pfaffia glomerata* plants (accession 22), under ambient (a[CO_2]) and elevated CO_2 concentration (e[CO_2]) and 20 consecutive days of well-watered and drought-stressed conditions. 20E content (mg g^{-1} DW) in (**a**) leaves, (**c**) stem, and (**e**) root. 20E production (**g**) in (**b**) leaves, (**d**) stem, and (**f**) root. Asterisks (*) indicate differences between CO_2 treatments within the same watering regime; hashtags (#) indicate differences between watering regimes within the same CO_2 supply by F test ($P \leq 0.05$). Data represent the mean of six biological replicates ($n = 6$) ± standard error. The ANOVA results showed a significant interaction between the factors ([CO_2] x watering regimes (WR)) for most variables; for details see Table S1

with [CO_2]-dependent drought tolerance under the controlled chamber conditions of this experiment. Specifically, CO_2 enrichment shifted biomass allocation responses under drought: a[CO_2]D favored increased root investment, whereas e[CO_2]D did not markedly alter root/shoot ratio, consistent with a scenario in which higher leaf-level WUE under e[CO_2] occurred in association with reduced stomatal conductance and less negative Ψ, rather than through mitigation of drought stress, partially reducing the need for allocation shifts toward roots.

Interestingly, another strategy is employed by *P. glomerata* under e[CO_2] to reprogram metabolic responses to water deficit. It should be noted that metabolite changes are expressed as relative variations, and large percentage increases do not necessarily imply high absolute concentrations. Rather, these shifts indicate coordinated metabolic reprogramming under drought and elevated

CO_2, independent of baseline metabolite pools. A remarkable increase in the content of soluble sugars was observed in plants exposed to e[CO_2]D. In addition to closing their stomata to prevent water loss through transpiration, plants acquire osmolytes, such as sugars, amino acids and proteins, to prevent turgor loss and protein denaturation. This mechanism favors the ability to withstand tissue dehydration and protects cellular functions under low water potentials (Hildebrandt 2018). In agreement, plants exposed to e[CO_2]D contained more glutamate, serine, and valine. Increased levels of these amino acids have been reported under drought conditions, contributing to osmotic adjustment (Ashrafi et al. 2018; Qiu et al. 2020). Heinemann et al. (2021) reported in Arabidopsis that drought stress-induced amino acid degradation delivers nitrogen and glutamate for the production of proline and GABA as osmolytes as well as alternative substrates for mitochondrial respiration. In addition, the carbon skeletons of some amino acids, such as leucine, lysine, valine, and serine are usually converted into precursors or intermediates of the tricarboxylic acid (TCA) cycle, directly feeding electrons into the mitochondrial electron transport chain, and consequently contributing to ATP production, which is crucial under stress conditions (Araújo et al. 2011b; Hildebrandt et al. 2015). Here, we posit that TCA cycle enzymes are positively regulated in drought-stressed plants, such as succinate dehydrogenase (cds.comp69239_c0_seq1; cds.comp69239_c0_seq1) and citrate synthase (cds.comp67529_c0_seq2; cds.comp66341_c1_seq1) (Tables **S2, S3**). Importantly, these osmotic and amino acid adjustments were most pronounced under e[CO_2]D, whereas a[CO_2]D showed comparatively limited shifts in the same metabolites (Table 1), supporting the conclusion that CO_2 enrichment modulated the metabolic configuration of drought responses rather than eliminating drought impacts.

In plants exposed to e[CO_2]D reduced levels of alanine and aspartate were observed. Nitrogen plays a central role in protein synthesis and e[CO_2] has a positive effect on nitrogen metabolism (Singh et al. 2015; Lee et al. 2020; Ebi et al. 2021). This effect is believed to be caused by stronger carbohydrate production, which increases the C/N ratio (Reich et al. 2006; Shi et al. 2016). Some studies showed that the source of assimilation and reduction of nitrogen (NO_3^- or NH_4^+) are influenced by e[CO_2] (Asensio et al. 2015; Andrews et al. 2020; Bloom et al. 2020). Maize plants exposed to e[CO_2]D also showed decreases in the amino acids alanine and aspartate, which correlated with nitrogen (Sicher and Barnaby 2012). In addition, proteome analysis revealed that e[CO_2] delayed or even eliminated many of the drought response proteins detected in plants grown under a[CO_2], such as plasma membrane-associated cation binding protein 1 (cds.comp26143_c0_seq1), glutathione S-transferase U17-like (cds.comp69177_c0_seq1), thioredoxin-like protein CDSP32 (cds.comp62233_c0_seq1), and various heat shock (cds.comp68654_c2_seq1; cds.comp27325_c0_seq1; cds.comp17310_c0_seq1; cds.comp65506_c0_seq1; and cds.comp25021_c0_seq1) proteins (Table S2). In addition, we observed more DAPs in almost all identified pathways (except amino sugar and nucleotide sugar metabolism) under a[CO_2]D than under e[CO_2]D. Taken together, these facts constitute circumstantial evidence that the metabolic responses to drought in plants under e[CO_2]D are modulated by carbon and nitrogen balance. From an environmental perspective, this CO_2-dependent modulation is relevant because atmospheric CO_2 is rising and drought frequency is expected to increase; therefore, understanding which stress traits are buffered, which are reprogrammed, and which remain constrained under e[CO_2] is central to predicting plant performance and specialized metabolite yield under future climates.

Drought and CO_2 Concentration and Interactions with Specialized Metabolism

Drought increased CAT and SOD activity regardless of [CO_2], consistent with reports that water limitation stimulates these enzymes (Abid et al. 2017; Sarker and Oba 2018; Jabeen et al. 2021). SOD converts superoxide (O_2^-) into hydrogen peroxide (H_2O_2), which is subsequently removed by CAT (Krishnamurthy and Wadhwani 2012). APX activity also increased under e[CO_2]D relative to a[CO_2]D and e[CO_2]WW. Given its high affinity for H_2O_2, APX facilitates its reduction across multiple cellular compartments using ascorbate as an electron donor (Sofo et al. 2015). Lipid peroxidation, measured indirectly through MDA accumulation (Khan and Panda 2007), rose under both a[CO_2]D and e[CO_2]D, indicating membrane damage. Thus, although e[CO_2] modulates antioxidant responses, it does not mitigate nor prevent drought-induced oxidative damage, in agreement with previous findings (Wu et al. 2022). Therefore, in this study, CO_2 enrichment altered the magnitude and configuration of antioxidant responses (e.g., APX induction under e[CO_2]D) without eliminating oxidative constraints imposed by drought, as indicated by elevated MDA under both CO_2 levels.

Under stressful conditions, plants can reprogram their primary metabolism towards the synthesis of secondary metabolites. For example, in the study by Felipe et al. (2019a, b), salinity stress increased 20E production, highlighting how stress can modulate primary metabolic pathways, thereby promoting the biosynthesis of secondary metabolites. Similarly, UV stress also triggered a comparable response, further reinforcing the interconnectedness between primary metabolism and the enhanced production

of secondary metabolites, such as 20E. Phenylpropanoids, including flavonoids and lignin, play essential roles in plant structure, function, and response to abiotic stress, and also contribute to the scavenging and elimination of ROS (Berni et al. 2019). In the phenylpropanoid pathway, several enzymes play crucial roles in lignin biosynthesis. Cinnamate 4-hydroxylase (C4H) catalyzes the hydroxylation of cinnamic acid, converting it to *p*-coumaric acid. The cafeoyl-CoA *O*-methyltransferase (CCoAOMT) catalyzes the methylation of caffeoyl-CoA, converting it into the corresponding methyl ester, which is typically known as feruloyl-CoA. In contrast, cinnamoyl-CoA reductase (CCR) converts feruloyl-CoA into coniferyl aldehyde. The cinnamyl alcohol dehydrogenase (CAD), converts coniferyl aldehyde to coniferyl alcohol. This enzymatic reaction is a key step in lignin synthesis, as coniferyl alcohol serves as an important precursor to produce lignin polymers (Wang et al. 2018; Ma et al. 2023).

Here, drought up-regulated *PgC4H*, *PgCCoAOMT*, and *PgCAD* under both [CO_2] conditions, whereas *PgCCR* was induced only under e[CO_2]D. All four genes showed higher expression in e[CO_2]D than in a[CO_2]D. Proteomic data further supported this pattern, with cinnamoyl-CoA reductase (CCR; cds.comp48028_c0_seq1) and caffeoyl-CoA O-methyltransferase (CCoAOMT; cds.comp47838_c0_seq1) accumulating under drought regardless of [CO_2] (Table S2). These results indicate that lignin-related pathways respond primarily to drought, with CO_2 enrichment acting as a modulatory signal that strengthens transcriptional activation without demonstrating a direct compensatory effect on drought-induced physiological impairment. Thus, while drought was the primary trigger, CO_2 enrichment superimposed a regulatory layer on lignin-related gene expression rather than providing functional mitigation of drought stress, indicating a CO_2-sensitive reprogramming of secondary metabolism.

Enhanced carbon assimilation under e[CO_2] may also affect 20E production. Although drought increased 20E content irrespective of [CO_2], only e[CO_2]D plants showed higher total 20E per plant, compensating for drought-induced biomass reduction. Drought increased 20E in leaves and stems under both [CO_2] treatments, but root 20E content rose significantly only under e[CO_2]D, suggesting that e[CO_2] may intensify 20E accumulation particularly in roots. While this requires further validation, these results indicate that drought is the primary trigger of 20E biosynthesis, whereas CO_2 enrichment modulates organ-level allocation and total yield rather than directly stimulating synthesis. This distinction addresses the apparent lack of a uniform CO_2 effect, as CO_2 enrichment did not replace drought as the driver of 20E induction but influenced whole-plant 20E output by modifying organ-level allocation and production under drought, which is directly relevant when evaluating medicinal metabolite yield under future atmospheric CO_2 scenarios.

Despite enhanced antioxidant enzyme activity, plants under e[CO_2]D exhibited greater oxidative stress, possibly due to excess ROS production and lower levels of antioxidants such as carotenoids, ascorbate-related proteins, and glutathione. The increased MDA content reinforces this interpretation. Elevated ROS may also have triggered 20E biosynthesis. Supporting this, 20E production in *P. glomerata* is known to increase under various abiotic stresses, including Zn exposure (Bernardy et al. 2020), UV-B radiation, and moderate salinity (Felipe et al. 2019a, b). Collectively, these findings underscore the interplay between drought, CO_2, ROS, antioxidant responses, lignin metabolism, and 20E biosynthesis. Importantly, CO_2 enrichment primarily reshaped the configuration and allocation of drought responses rather than alleviating core drought constraints, highlighting the need to interpret specialized metabolism outcomes jointly with persistent physiological stress under future climate scenarios.

The Role of Cytochrome P450 Proteins in Lignin Biosynthesis and 20E Production

In our study, we observed a significant positive regulation of the *PgC4H* gene, which encodes the CYP73A protein, in *P. glomerata* plants grown under drought conditions. Additionally, we detected the accumulation of the CYP72A219-like protein (cds.comp18142_c0_seq1) specifically under the e[CO_2]D (Table S2). The *C4H* gene is known to be involved in lignin biosynthesis, as previously mentioned. The function of the CYP72A219 protein remains poorly understood, though previous studies in other plant species have provided some insights. For example, in *Amaranthus palmeri*, *CYP72A219* was consistently highly expressed in all glufosinate herbicide-tolerant biotypes (Salas-Perez et al. 2018). This suggests that the CYP72A219 protein may play a role in the metabolism and detoxification of herbicides. *CYP72A219* of *Panax ginseng* is one of the genes possibly responsible for ginsenoside biosynthesis. Ginsenosides are important secondary metabolites in ginseng plants, and they are known for their various health benefits. CYP72A219 of *Panax ginseng* has been proposed as one of the genes involved in ginsenoside biosynthesis, a class of sterol-derived secondary metabolites (Han et al. 2011; Li et al. 2021). These findings suggest a potential role of CYP72A219 in secondary metabolism and stress-associated metabolic reprogramming, rather than a direct adaptive or protective function. In the context of our factorial treatments, the CO_2 signal appears relevant because this protein accumulated specifically under e[CO_2]D, indicating that

CO_2 enrichment may contribute to activating or stabilizing a sterol-related P450 node during drought, without implying a compensatory mitigation of drought-induced physiological impairment, even when several other stress-associated proteins were attenuated under e[CO_2].

De novo assembly of the *P. glomerata* transcriptome revealed several genes from the CYPs P450 family related to secondary metabolism and stress (Batista et al. 2019a). *Phantom* (CYP76C) was directly correlated with 20E content, suggesting its participation in the 20E biosynthesis pathway (Batista et al. 2019a). Additionally, studies have shown that UV-B radiation and moderate salt stress can increase 20E levels in *P. glomerata*. These stress conditions have been shown to upregulate the expression of the *Spook* (CYP83A) and *Phantom* genes (Felipe et al. 2019a, b). Here, we observed a predicted interaction between the CYP72A219-like protein and five regulatory proteins of the sterol biosynthetic pathway (Figs. 6c and **S7**). This interaction supports a role for CYP72A219-like proteins in drought-associated metabolic reconfiguration under elevated CO_2, rather than establishing a direct causal link to enhanced stress tolerance or drought mitigation. Considering the putative participation of CYP72A219-like protein in sterol-derived secondary metabolism and its association with antioxidant-related pathways, it is plausible that ROS signaling contributes to the modulation of 20E biosynthesis during drought stress, although this interpretation remains associative. Further functional validation is required to determine whether this protein plays a regulatory, permissive, or downstream role in 20E accumulation under combined drought and CO_2 enrichment.

Our findings show that *P. glomerata* exhibits coordinated physiological, metabolic, and molecular adjustments to drought that are modulated by CO_2 concentration, within the constraints imposed by the controlled chamber-level experimental design. This is the first study to demonstrate how drought interacts with CO_2 availability to regulate secondary metabolism and the production of 20E. Comparative proteomic analysis identified 405 common DAPs associated with 19 metabolic pathways, notably porphyrin metabolism, carbon metabolism, amino acid biosynthesis, and cofactor biosynthesis. Elevated CO_2 (e[CO_2]) markedly affected drought-responsive proteins, delaying or suppressing several responses typically observed under a[CO_2]. Under e[CO_2] combined with drought (e[CO_2]D), plants reprogrammed primary metabolism toward secondary metabolite biosynthesis. Drought upregulated key lignin pathway genes (*PgC4H*, *PgCCoAOMT*, *PgCCR*, and *PgCAD*), with consistently higher expression under e[CO_2]D than a[CO_2]D. Drought also enhanced antioxidant enzyme activity and increased 20E levels in leaves and stems under both CO_2 conditions. However, only e[CO_2]D elevated 20E levels in roots and stimulated its synthesis in both leaves and roots, indicating a redistribution and reallocation of metabolic investment rather than a complete alleviation of drought stress. Overall, the data support the conclusion that CO_2 enrichment influenced selected physiological, metabolic, and proteomic endpoints mainly by reshaping drought response intensity and allocation patterns. Conversely, core drought constraints on growth and photosynthesis persisted. This integrated interpretation reinforces the relevance of CO_2–drought interactions for predicting secondary metabolite dynamics under future climate scenarios.

Supplementary Information The online version contains supplementary material available at https://doi.org/10.1007/s00344-026-12117-y.

Acknowledgements We thank Prof. Takeshi Kamada (Universidade de Rio Verde, Rio Verde, GO, Brazil), Dr. Roberto Fontes Vieira, and Dr. Rosa Belém Alves Neves (National Center for Genetic Resources and Biotechnology, Embrapa/Cenargen, Brasília, DF, Brazil) for providing *Pfaffia glomerata* accessions. The Department of Plant Biology and Biochemistry and Molecular Biology, Universidade Federal de Viçosa (UFV), is gratefully acknowledged for providing facilities for physiological, biochemical, structural, and molecular. The authors are grateful to the Laboratory for Molecular Genetics of Bacteria (Bioagro/UFV) for providing facilities for quantitative real-time PCR analysis. Proteomic analyses were performed at the Laboratory of Cell and Tissue Biology and Biotechnology, Universidade Estadual do Norte Fluminense, Darcy Ribeiro. The Plant Metabolism and Metabolomics Laboratory from the Institute of Plant Biochemistry, Heinrich Heine University Düsseldorf, which was used to analyze the metabolites quantified by GC-MS is supported by the Deutsche Forschungsgemeinschaft (DFG, German Research Foundation) under Germany´s Excellence Strategy – EXC-2048/1 –project ID 390686111. The Coordenação de Aperfeiçoamento de Pessoal de Nível Superior—Brazil (CAPES)—Funding Code 001, the Fundação de Amparo à Pesquisa do Estado de Minas Gerais [FAPEMIG; APQ-00772-19, APQ-01433-22, and RED-00060-23—Rede Mineira em Fisiologia de Plantas sob Condições de Estresse (Rede Mineira Estresse em Plantas) and scholarship to MM—BCTI-II RED-00060-23], and the Conselho Nacional de Desenvolvimento Científico e Tecnológico (CNPq; Grant Nos. 313901/2018-0, 407276/2021-1 and 406455/2022-8) are gratefully acknowledged for providing scholarships and financial support. We would like to thank Editage (www.editage.com) for English language editing.

Author Contribution TDS, DSB, SHSF, ANN, and WCO designed the study; TDS and KJMR performed most of the experiments; TDS, KJMR, EAF, MM, LMF, and MTA performed physiological and biochemical analyses; TDS performed structural and molecular analyses; TDS, TRO, CSC, and VS performed proteomic analyses; TDS, MM, PW, and APMW performed metabolic analyses; TDS and TRO analyzed the data; TDS, EAF, SHSF, DSB, ANN, and WCO wrote the article with input from all other authors. All authors have read and approved the final manuscript.

Funding The Article Processing Charge (APC) for the publication of this research was funded by the Coordenação de Aperfeiçoamento de Pessoal de Nível Superior - Brasil (CAPES) (ROR identifier: 00x0ma614). Deutsche Forschungsgemeinschaft, EXC-2048/1 – Project ID 390686111 (Andreas P. M. Weber), Coordenação de Aperfeiçoamento de Pessoal de Nível Superior (CAPES)—Funding Code

001, Fundação de Amparo à Pesquisa do Estado de Minas Gerais (FAPEMIG), RED-00060-23—Rede Mineira em Fisiologia de Plantas sob Condições de Estresse (Rede Mineira Estresse em Plantas) (Adriano Nunes-Nesi), Conselho Nacional de Desenvolvimento Científico e Tecnológico, Grant 406455/2022-8 / INCT—Fisiologia do Estresse (Adriano Nunes-Nesi), and Grant No. CNPq/PQ 313901/2018-0 (Wagner Campos Otoni).

Data aAvailability All data used for the analyses in this study are publicly accessible. Raw mass spectrometry proteomic data files were deposited with the ProteomeXchange consortium via the PRIDE partner repository under the accession number PXD040626.

Declarations

Conflict of Interest The authors declare that there is no conflict of interest.

Open Access This article is licensed under a Creative Commons Attribution 4.0 International License, which permits use, sharing, adaptation, distribution and reproduction in any medium or format, as long as you give appropriate credit to the original author(s) and the source, provide a link to the Creative Commons licence, and indicate if changes were made. The images or other third party material in this article are included in the article's Creative Commons licence, unless indicated otherwise in a credit line to the material. If material is not included in the article's Creative Commons licence and your intended use is not permitted by statutory regulation or exceeds the permitted use, you will need to obtain permission directly from the copyright holder. To view a copy of this licence, visit http://creativecommons.org/licenses/by/4.0/.

References

AbdElgawad H, Zinta G, Hornbacher J et al (2023) Elevated CO_2 mitigates the impact of drought stress by upregulating glucosinolate metabolism in *Arabidopsis thaliana*. Plant Cell Environ. https://doi.org/10.1111/pce.14521

Abid G, M'hamdi M, Mingeot D et al (2017) Effect of drought stress on chlorophyll fluorescence, antioxidant enzyme activities and gene expression patterns in faba bean (*Vicia faba* L.). Arch Agron Soil Sci. https://doi.org/10.1080/03650340.2016.1224857

Al Jaouni S, Saleh AM, Wadaan MAM et al (2018) Elevated CO_2 induces a global metabolic change in basil (*Ocimum basilicum* L.) and peppermint (*Mentha piperita* L.) and improves their biological activity. J Plant Physiol. https://doi.org/10.1016/j.jplph.2018.03.016

Almuhayawi MS, Hassan AHA, Al Jaouni SK et al (2021) Influence of elevated CO_2 on nutritive value and health-promoting prospective of three genotypes of alfalfa sprouts (*Medicago sativa*). Food Chem. https://doi.org/10.1016/j.foodchem.2020.128147

Andrews M, Condron LM, Kemp PD et al (2020) Will rising atmospheric CO_2 concentration inhibit nitrate assimilation in shoots but enhance it in roots of C3 plants? Physiol Plant. https://doi.org/10.1111/ppl.13096

Araújo WL, Nunes-Nesi A, Osorio S et al (2011a) Antisense inhibition of the iron-sulphur subunit of succinate dehydrogenase enhances photosynthesis and growth in tomato via an organic acid-mediated effect on stomatal aperture. Plant Cell. https://doi.org/10.1105/tpc.110.081224

Araújo WL, Nunes-Nesi A, Fernie AR et al (2011b) Protein degradation-an alternative respiratory substrate for stressed plants. Trends Plant Sci. https://doi.org/10.1016/j.tplants.2011.05.008

Asensio JS, Rachmilevitch S, Bloom AJ (2015) Responses of Arabidopsis and wheat to rising CO_2 depend on nitrogen source and nighttime CO_2 levels. Plant Physiol. https://doi.org/10.1104/pp.15.00110

Ashrafi M, Azimi-Moqadam MR, Moradi P et al (2018) Effect of drought stress on metabolite adjustments in drought tolerant and sensitive thyme. Plant Physiol Biochem. https://doi.org/10.1016/j.plaphy.2018.09.009

Ávila RT, Cardoso AA, Almeida WL et al (2020) Coffee plants respond to drought and elevated [CO_2] through changes in stomatal function, plant hydraulic conductance, and aquaporin expression. Environ Exp Bot. https://doi.org/10.1016/j.envexpbot.2020.104148

Bakrim A, Maria A, Sayah F et al (2008) Ecdysteroids in spinach (*Spinacia oleracea* L.): biosynthesis, transport and regulation of levels. Plant Physiol Biochem. https://doi.org/10.1016/j.plaphy.2008.06.002

Bates LS, Waldren RP, Teare ID (1973) Rapid determination of free proline for water-stress studies. Plant Soil. https://doi.org/10.1007/bf00018060

Batista DS, Dias LLC, Rêgo MM et al (2017) Flask sealing on in vitro seed germination and morphogenesis of two types of ornamental pepper explants. Cienc Rural. https://doi.org/10.1590/0103-8478cr20150245

Batista DS, Koehler AD, Romanel E et al (2019a) De novo assembly and transcriptome of *Pfaffia glomerata* uncovers the role of photoautotrophy and the P450 family genes in 20-hydroxyecdysone production. Protoplasma. https://doi.org/10.1007/s00709-018-1322-1

Batista DS, Moreira VS, Felipe SHS et al (2019b) Reference gene selection for qRT-PCR in Brazilian-ginseng [*Pfaffia glomerata* (Spreng.) Pedersen] as affected by various abiotic factors. Plant Cell Tissue Organ Cult. https://doi.org/10.1007/s11240-019-01606-6

Batista-Silva W, Heinemann B, Rugen N et al (2019) The role of amino acid metabolism during abiotic stress release. Plant Cell Environ. https://doi.org/10.1111/pce.13518

Bernardy K, Farias JG, Pereira AS et al (2020) Plants' genetic variation approach applied to zinc contamination: secondary metabolites and enzymes of the antioxidant system in *Pfaffia glomerata* accessions. Chemosphere. https://doi.org/10.1016/j.chemosphere.2020.126692

Berni R, Luyckx M, Xu X et al (2019) Reactive oxygen species and heavy metal stress in plants: impact on the cell wall and secondary metabolism. Environ Exp Bot. https://doi.org/10.1016/j.envexpbot.2018.10.017

Birami B, Thomas N, Gattmann M et al (2020) Hot drought reduces the effects of elevated CO_2 on tree water-use efficiency and carbon metabolism. New Phytol. https://doi.org/10.1111/nph.16471

Bloom AJ, Kasemsap P, Rubio-Asensio JS (2020) Rising atmospheric CO_2 concentration inhibits nitrate assimilation in shoots but enhances it in roots of C3 plants. Physiol Plant. https://doi.org/10.1111/ppl.13040

Bradford MM (1976) A rapid and sensitive method for the quantitation of microgram quantities of protein utilizing the principle of protein-dye binding. Anal Biochem. https://doi.org/10.1016/0003-2697(76)90527-3

Buniam J, Chukijrungroat N, Rattanavichit Y et al (2020) 20-hydroxyecdysone ameliorates metabolic and cardiovascular dysfunction in high-fathigh-fructose-fed ovariectomized rats. BMC Complement Med Ther. https://doi.org/10.1186/s12906-020-02936-1

Chance B, Maehly AC (1955) Assay of catalases and peroxidases. Methods Enzym. https://doi.org/10.1016/S0076-6879(55)02300-8

Choi HS, Koo H, Bin Jeon SW et al (2022) Modification of ginsenoside saponin composition via the CRISPR/Cas9-mediated knockout of

protopanaxadiol 6-hydroxylase gene in *Panax ginseng*. J Ginseng Res. https://doi.org/10.1016/j.jgr.2021.06.004
Corrêa JPO, Vital CE, Pinheiro MVM et al (2015) In vitro photoautotrophic potential and ex vitro photosynthetic competence of *Pfaffia glomerata* (Spreng.) Pedersen accessions. Plant Cell Tissue Organ Cult. https://doi.org/10.1007/s11240-014-0700-4
Cruz CD (2016). Genes Software – extended and integrated with the R, Matlab and Selegen. Acta Sci. Agron.https://doi.org/10.4025/actasciagron.v38i3.32629
Dinan L, Mamadalieva NZ, Lafont R (2020) Dietary phytoecdysteroids. In: Xiao J, Sarker SD, Asakawa Y (eds) Handbook of dietary phytochemicals. Springer Nature Singapore Pte Ltd., Singapore, pp 1–54. https://doi.org/10.1007/978-981-13-1745-3_35-1
Dinan L, Balducci C, Guibout L et al (2021) Ecdysteroid metabolism in mammals: the fate of ingested 20-hydroxyecdysone in mice and rats. J Steroid Biochem Mol Biol. https://doi.org/10.1016/j.jsbmb.2021.105896
Distler U, Kuharev J, Navarro P (2014) Drift time-specific collision energies enable deep-coverage data-independent acquisition proteomics. Nat Methods. https://doi.org/10.1038/nmeth.2767
Dusenge ME, Duarte AG, Way DA (2019) Plant carbon metabolism and climate change: elevated CO_2 and temperature impacts on photosynthesis, photorespiration and respiration. New Phytol. https://doi.org/10.1111/nph.15283
Ebi KL, Anderson CL, Hess JJ et al (2021) Nutritional quality of crops in a high CO_2 world: an agenda for research and technology development. Environ Res Lett. https://doi.org/10.1088/1748-9326/abfcfa
Felipe SHS, Batista DS, Chagas K et al (2019a) Accessions of Brazilian ginseng (*Pfaffia glomerata*) with contrasting anthocyanin content behave differently in growth, antioxidative defense, and 20-hydroxyecdysone levels under UV-B radiation. Protoplasma. https://doi.org/10.1007/s00709-019-01400-3
Felipe SHS, Batista DS, Vital CE et al (2019b) Salinity-induced modifications on growth, physiology and 20-hydroxyecdysone levels in Brazilian-ginseng [*Pfaffia glomerata* (Spreng.) Pedersen]. Plant Physiol Biochem. https://doi.org/10.1016/j.plaphy.2019.05.002
Fernie AR, Roscher A, Ratcliffe RG et al (2001) Fructose 2,6-bisphosphate activates pyrophosphate: fructose-6-phosphate 1-phosphotransferase and increases triose phosphate to hexose phosphate cycling in heterotrophic cells. Planta. https://doi.org/10.1007/s004250000386
Ferreira PRB, da Cruz ACF, Batista DS et al (2019) CO_2 enrichment and supporting material impact the primary metabolism and 20-hydroxyecdysone levels in Brazilian ginseng grown under photoautotrophy. Plant Cell Tissue Organ Cult. https://doi.org/10.1007/s11240-019-01664-w
Fiehn O (2007) Validated high quality automated metabolome analysis of *Arabidopsis thaliana* leaf disks. Concepts in plant metabolomics. Springer Netherlands, Dordrecht, pp 1–18. https://doi.org/10.1007/978-1-4020-5608-6_1
Fortini EA, Batista DS, Felipe SHS et al (2023) Physiological, epigenetic, and proteomic responses in *Pfaffia glomerata* growth in vitro under salt stress and 5-azacytidine. Protoplasma. https://doi.org/10.1007/s00709-022-01789-4
Franco RR, Takata LA, Chagas K et al (2021) A 20-hydroxyecdysone-enriched fraction from *Pfaffia glomerata* (Spreng.) Pedersen roots alleviates stress, anxiety, and depression in mice. J Ethnopharmacol. https://doi.org/10.1016/j.jep.2020.113599
Giannopolitis CN, Ries SK (1977) Superoxide dismutases. Plant Physiol. https://doi.org/10.1104/pp.59.2.309
Gibon Y, Bläsing OE, Palacios-Rojas N et al (2004) Adjustment of diurnal starch turnover to short days: depletion of sugar during the night leads to a temporary inhibition of carbohydrate utilization, accumulation of sugars and post-translational activation of ADP-glucose pyrophosphorylase in the following light period. Plant J. https://doi.org/10.1111/j.1365-313X
Gu J, Weber K, Klemp E et al (2012) Identifying core features of adaptive metabolic mechanisms for chronic heat stress attenuation contributing to systems robustness. Integr Biol. https://doi.org/10.1039/c2ib00109h
Guo S, Tian Z, Wu QW et al (2021) Steroid hormone ecdysone deficiency stimulates preparation for photoperiodic reproductive diapause. PLoS Genet. https://doi.org/10.1371/journal.pgen.1009352
Han JY, Kim HJ, Kwon YS et al (2011) The Cyt P450 enzyme CYP716A47 catalyzes the formation of protopanaxadiol from dammarenediol-II during ginsenoside biosynthesis in *Panax ginseng*. Plant Cell Physiol. https://doi.org/10.1093/pcp/pcr150
Han JY, Baek S-H, Jo HJ et al (2019) Genetically modified rice produces ginsenoside aglycone (protopanaxadiol). Planta. https://doi.org/10.1007/s00425-019-03204-4
Hatfield JL, Dold C (2019) Water-use efficiency: advances and challenges in a changing climate. Front Plant Sci. https://doi.org/10.3389/fpls.2019.00103
Havaux M, Tardy F (1999) Loss of chlorophyll with limited reduction of photosynthesis as an adaptive response of Syrian barley landraces to high-light and heat stress. Aust J Plant Physiol. https://doi.org/10.1071/PP99046
Havir EA, McHale NA (1987) Biochemical and developmental characterization of multiple forms of catalase in tobacco leaves. Plant Physiol. https://doi.org/10.1104/pp.84.2.450
Heath RL, Packer L (1968) Photoperoxidation in isolated chloroplasts. Arch Biochem Biophys. https://doi.org/10.1016/0003-9861(68)90654-1
Heinemann B, Künzler P, Eubel H et al (2021) Estimating the number of protein molecules in a plant cell: protein and amino acid homeostasis during drought. Plant Physiol. https://doi.org/10.1093/plphys/kiaa050
Hildebrandt TM (2018) Synthesis versus degradation: directions of amino acid metabolism during Arabidopsis abiotic stress response. Plant Mol Biol. https://doi.org/10.1007/s11103-018-0767-0
Hildebrandt TM, Nesi AN, Araújo WL et al (2015) Amino acid catabolism in plants. Mol Plant. https://doi.org/10.1016/j.molp.2015.09.005
Houshmandfar A, Fitzgerald GJ, Tausz M (2015) Elevated CO_2 decreases both transpiration flow and concentrations of Ca and Mg in the xylem sap of wheat. J Plant Physiol. https://doi.org/10.1016/j.jplph.2014.10.008
Hozzein WN, Saleh AM, Habeeb TH et al (2020) CO_2 treatment improves the hypocholesterolemic and antioxidant properties of fenugreek seeds. Food Chem. https://doi.org/10.1016/j.foodchem.2019.125661
Hsu PK, Takahashi Y, Munemasa S et al (2018) Abscisic acid-independent stomatal CO_2 signal transduction pathway and convergence of CO_2 and ABA signaling downstream of OST1 kinase. Proc Natl Acad Sci U S A. https://doi.org/10.1073/pnas.1809204115
Iarema L, Cruz ACF, Saldanha CW et al (2012) Photoautotrophic propagation of Brazilian ginseng [*Pfaffia glomerata* (Spreng.) Pedersen]. Plant Cell Tissue Organ Cult. https://doi.org/10.1007/s11240-012-0145-6
IPCC. (2014). Climate change 2014: impacts, adaptation, and vulnerability. 485–533.
Iqbal S, Wang X, Mubeen I et al (2022) Phytohormones trigger drought tolerance in crop plants: outlook and future perspectives. Front Plant Sci. https://doi.org/10.3389/fpls.2021.799318
Jabeen M, Akram NA, Ashraf M et al (2021) Thiamin stimulates growth and secondary metabolites in turnip (*Brassica rapa* L.) leaf and root under drought stress. Physiol Plant. https://doi.org/10.1111/ppl.13215

Janeczko A, Oklestkova J, Tarkowská D et al (2021) Naturally occurring ecdysteroids in *Triticum aestivum* L. and evaluation of fenarimol as a potential inhibitor of their biosynthesis in plants. Int J Mol Sci. https://doi.org/10.3390/ijms22062855

Karnovsky MJ (1964) A formaldehyde-glutaraldehyde fixative of high osmolality for use in electron microscopy. J Cell Biol 27:1A-149A

Khan MH, Panda SK (2007) Alterations in root lipid peroxidation and antioxidative responses in two rice cultivars under NaCl-salinity stress. Acta Physiol Plant. https://doi.org/10.1007/s11738-007-0093-7

Krämer U, Pickering IJ, Weiss DJ (2022) Root-to-shoot signaling and systemic acquired acclimation. Front Plant Sci. https://doi.org/10.3389/fpls.2022.897924

Krishnamurthy P, Wadhwani A (2012) Antioxidant enzymes and human health. Antioxid Enzyme. https://doi.org/10.5772/48109

Lafont R (1997) Ecdysteroids and related molecules in animals and plants. Arch Insect Biochem Physiol. https://doi.org/10.1002/(SICI)1520-6327(1997)35:1/2%3c3::AID-ARCH2%3e3.0.CO;2-X

Lee YH, Sang WG, Baek JK et al (2020) The effect of concurrent elevation in CO_2 and temperature on the growth, photosynthesis, and yield of potato crops. PLoS ONE. https://doi.org/10.1371/journal.pone.0241081

Lei H, Zhang H, Zhang Z et al (2023) Physiological and transcriptomic analyses of roots from *Panax ginseng* C. A. Meyer under drought stress. Ind Crops Prod. https://doi.org/10.1016/j.indcrop.2022.115858

Li P, Li H, Zong Y et al (2017) Photosynthesis and metabolite responses of *Isatis indigotic*a Fortune to elevated [CO_2]. Crop J. https://doi.org/10.1016/j.cj.2017.03.007

Li D, Zhang X, Li L et al (2019) Elevated CO_2 delayed the chlorophyll degradation and anthocyanin accumulation in postharvest strawberry fruit. Food Chem. https://doi.org/10.1016/j.foodchem.2019.01.150

Li Y, Kong D, Fu Y et al (2020) The effect of developmental and environmental factors on secondary metabolites in medicinal plants. Plant Physiol. https://doi.org/10.1016/j.plaphy.2020.01.006

Li X, Cheng X, Liao B et al (2021) Spatial protein expression of *Panax ginseng* by in-depth proteomic analysis for ginsenoside biosynthesis and transportation. J Ginseng Res. https://doi.org/10.1016/j.jgr.2020.01.009

Lima ALS, DaMatta FM, Pinheiro HÁ et al (2002) Photochemical responses and oxidative stress in two clones of *Coffea canephora* under water deficit conditions. Environ Exp Bot. https://doi.org/10.1016/S0098-8472(01)00130-7

Lin X, Smagghe G (2019) Roles of the insulin signaling pathway in insect development and organ growth. Peptides. https://doi.org/10.1016/j.peptides.2018.02.001

Lisec J, Schauer N, Kopka J et al (2006) Gas chromatography mass spectrometry-based metabolite profiling in plants. Nat Protoc. https://doi.org/10.1038/nprot.2006.59

Livak KJ, Schmittgen TD (2001) Analysis of relative gene expression data using real-time quantitative PCR and the $2^{-\Delta\Delta CT}$ method. Methods. https://doi.org/10.1006/meth.2001.1262

Louback E, Batista DS, Pereira TAR et al (2021) CO_2 enrichment leads to altered cell wall composition in plants of *Pfaffia glomerata* (Spreng.) Pedersen (Amaranthaceae). Plant Cell Tissue Organ Cult. https://doi.org/10.1007/s11240-021-02031-4

Lv C, Huang Y, Sun W et al (2022) Elevated [CO_2] raises the temperature optimum of photosynthesis and thus promotes net photosynthesis of winter wheat and rice. Physiol Plant. https://doi.org/10.1111/ppl.13757

Ma J, Li X, He M et al (2023) A joint transcriptomic and metabolomic analysis reveals the regulation of shading on lignin biosynthesis in *Asparagus*. Int J Mol Sci. https://doi.org/10.3390/ijms24021539

De la Mata L, Cabello P, De la Haba P et al (2012) Growth under elevated atmospheric CO2 concentration accelerates leaf senescence in sunflower (*Helianthus annuus* L.) plants. J Plant Physiol. https://doi.org/10.1016/j.jplph.2012.05.024

Marchioretto MS, Miotto STS, Siqueira C (2010) O gênero *Pfaffia* Mart (Amaranthaceae) no Brasil. Hoehnea 37(3):461–511

Mehmood I, Bari A, Irshad S et al (2020) Climate change forecasting and modeling for the year of 2050. Environment, climate, plant and vegetation growth. Springer International Publishing, Cham, pp 109–122. https://doi.org/10.1007/978-3-030-49732-3_5

Murashige T, Skoog F (1962) A revised medium for rapid growth and bio assays with tobacco tissue cultures. Physiol Plant. https://doi.org/10.1111/j.1399-3054.1962.tb08052.x

Nakano Y, Asada K (1981) Hydrogen peroxide is scavenged by ascorbate-specific peroxidase in spinach chloroplasts. Plant Cell Physiol. https://doi.org/10.1093/oxfordjournals.pcp.a076232

Neff MM, Chory J (1998) Genetic interactions between Phytochrome A, Phytochrome B, and Cryptochrome 1 during *Arabidopsis* development. Plant Physiol 118:27–35. https://doi.org/10.1104/pp.118.1.27

Neves CS, Gomes SSL, Santos TR et al (2016) Brazilian ginseng" (*Pfaffia glomerata* Spreng. Pedersen, Amaranthaceae) methanolic extract: Cytogenotoxicity in animal and plant assays. S Afr J Bot. https://doi.org/10.1016/j.sajb.2016.07.003

Nunes-Nesi A, Carrari F, Gibon Y et al (2007) Deficiency of mitochondrial fumarase activity in tomato plants impairs photosynthesis via an effect on stomatal function. Plant J. https://doi.org/10.1111/j.1365-313X.2007.03115.x

O'Brien TP, McCully ME (1981) The study of plant structure principles and selected methods. Termarcarphi Pty. Ltd., Melb, p 581

Oliveira TR, Balfagón D, Sousa KR et al (2022) Long-term subculture affects rooting competence via changes in the hormones and protein profiles in *Cedrela fissilis* Vell. (Meliaceae) shoots. Plant Cell Tissue Organ Cult. https://doi.org/10.1007/s11240-021-02172-6

Pazzagli PT, Weiner J, Liu F (2016) Effects of CO_2 elevation and irrigation regimes on leaf gas exchange, plant water relations, and water use efficiency of two tomato cultivars. Agric Water Manag. https://doi.org/10.1016/j.agwat.2016.02.015

Perez-Riverol Y, Bai J, Bandla C et al (2022) The PRIDE database resources in 2022: a hub for mass spectrometry-based proteomics evidences. Nucleic Acids Res. https://doi.org/10.1093/nar/gkab1038

Porra RJ, Thompson WA, Kriedemann PE (1989) Determination of accurate extinction coefficients and simultaneous equations for assaying chlorophylls a and b extracted with four different solvents: verification of the concentration of chlorophyll standards by atomic absorption spectroscopy. Biochim Biophys Acta Bioenerg. https://doi.org/10.1016/S0005-2728(89)80347-0

Qiao Y, Zhang H, Dong B et al (2010) Effects of elevated CO_2 concentration on growth and water use efficiency of winter wheat under two soil water regimes. Agric Water Manag. https://doi.org/10.1016/j.agwat.2010.06.007

Qiu XM, Sun YY, Ye XY et al (2020) Signaling role of glutamate in plants. Front Plant Sci. https://doi.org/10.3389/fpls.2019.01743

Rajanayake KK, Boldt JK, Isailovic D (2021) Elevated carbon dioxide and chronic warming together decrease nitrogen uptake rate, net translocation, and assimilation in tomato. Plants Basel. https://doi.org/10.3390/plants10040722

Reich PB, Hungate BA, Luo Y (2006) Carbon-nitrogen interactions in terrestrial ecosystems in response to rising atmospheric carbon dioxide. Annu Rev Ecol Evol Syst. https://doi.org/10.2307/annurev.ecolsys.37.091305.30000023

Reis RS, Vale EM, Sousa KR et al (2021) Pretreatment free of 2,4-dichlorophenoxyacetic acid improves the differentiation of sugarcane somatic embryos by affecting the hormonal balance

and the accumulation of reserves. Plant Cell Tissue Organ Cult. https://doi.org/10.1007/s11240-020-01995-z

Ribeiro STC, Gancedo NC, Braz de Oliveira AJ et al (2024) A comprehensive review of *Pfaffia glomerata* botany, ethnopharmacology, phytochemistry, biological activities, and biotechnology. J Ethnopharmacol 328:118003. https://doi.org/10.1016/j.jep.2024.118003

Roy S, Mathur P (2021) Delineating the mechanisms of elevated CO_2 mediated growth, stress tolerance and phytohormonal regulation in plants. Plant Cell Rep. https://doi.org/10.1007/s00299-021-02738-w

Salas-Perez RA, Saski CA, Noorai RE et al (2018) RNA-Seq transcriptome analysis of *Amaranthus palmeri* with differential tolerance to glufosinate herbicide. PLoS ONE. https://doi.org/10.1371/journal.pone.0195488

Saldanha CW, Otoni CG, Notini MM et al (2013) A CO_2-enriched atmosphere improves in vitro growth of Brazilian ginseng [*Pfaffia glomerata* (Spreng.) Pedersen]. In Vitro Cell Dev Biol - Plant. https://doi.org/10.1007/s11627-013-9529-5

Saldanha CW, Otoni CG, Rocha DI et al (2014) CO_2-enriched atmosphere and supporting material impact the growth, morphophysiology and ultrastructure of in vitro Brazilian-ginseng [*Pfaffia glomerata* (Spreng.) Pedersen] plantlets. Plant Cell Tissue Organ Cult. https://doi.org/10.1007/s11240-014-0464-x

Sarker U, Oba S (2018) Catalase, superoxide dismutase and ascorbate-glutathione cycle enzymes confer drought tolerance of *Amaranthus tricolor*. Sci Rep. https://doi.org/10.1038/s41598-018-34944-0

Scholander PF, Hammel HT, Hemmingsen EA (1964) Hydrostatic pressure and osmotic potential in leaves of mangroves and some other plants. Proc Natl Acad Sci USA. https://doi.org/10.1073/pnas.52.1.119

Schneider C, Rasband W, Eliceiri K (2012) NIH Image to ImageJ: 25 years of image analysis. Nat Methods. https://doi.org/10.1038/nmeth.2089

Sekhar KM, Reddy KSR, Reddy AR (2023) Photosynthesis and carbon sequestration efficacy of *Conocarpus erectus* L. (Combretaceae) grown under elevated CO_2 atmosphere. Plant Physiol Rep. https://doi.org/10.1007/s40502-022-00702-8

Shi Z, Yang Y, Zhou X et al (2016) Inverse analysis of coupled carbon-nitrogen cycles against multiple datasets at ambient and elevated CO_2. J Plant Ecol. https://doi.org/10.1093/jpe/rtv059

Shim SH, Lee SK, Lee DW et al (2020) Loss of function of rice plastidic glycolate/glycerate translocator 1 impairs photorespiration and plant growth. Front Plant Sci. https://doi.org/10.3389/fpls.2019.01726

Shinohara T, Leskovar DI (2014) Effects of ABA, antitranspirants, heat and drought stress on plant growth, physiology and water status of artichoke transplants. Sci Hortic. https://doi.org/10.1016/j.scienta.2013.10.045

Sicher RC, Barnaby JY (2012) Impact of carbon dioxide enrichment on the responses of maize leaf transcripts and metabolites to water stress. Physiol Plant. https://doi.org/10.1111/j.1399-3054

Silva TD, Chagas K, Batista DS et al (2019) Morphophysiological in vitro performance of Brazilian ginseng (*Pfaffia glomerata* (Spreng.) Pedersen) based on culture medium formulations. In Vitro Cell Dev Biol Plant. https://doi.org/10.1007/s11627-019-10003-9

Silva TD, Batista DS, Fortini EA et al (2020) Blue and red light affects morphogenesis and 20-hydroxyecdisone content of *in vitro Pfaffia glomerata* accessions. J Photochem Photobiol B. https://doi.org/10.1016/j.jphotobiol.2019.111761

Silva TD, Batista DS, Castro KM et al (2021) Irradiance-driven 20-hydroxyecdysone production and morphophysiological changes in *Pfaffia glomerata* plants grown in vitro. Protoplasma. https://doi.org/10.1007/s00709-020-01558-1

Singh A, Pandey B, Kumari S et al (2015) Nitrogen availability modulates CO_2-induced responses of *Catharanthus roseus*: biomass allocation, carbohydrates and alkaloids profile. J Appl Res Med Aromat Plants. https://doi.org/10.1016/j.jarmap.2015.07.002

Soares JC, Santos CS, Carvalho SMP et al (2019) Preserving the nutritional quality of crop plants under a changing climate: importance and strategies. Plant Soil. https://doi.org/10.1007/s11104-019-04229-0

Sofo A, Scopa A, Nuzzaci M et al (2015) Ascorbate peroxidase and catalase activities and their genetic regulation in plants subjected to drought and salinity stresses. Int J Mol Sci. https://doi.org/10.3390/ijms160613561

Song H, Li Y, Xu X et al (2020) Analysis of genes related to chlorophyll metabolism under elevated CO_2 in cucumber (*Cucumis sativus* L.). Sci Hortic. https://doi.org/10.1016/j.scienta.2019.108988

Szklarczyk D, Gable AL, Nastou KC et al (2021) Correction to 'the STRING database in 2021: customizable protein–protein networks, and functional characterization of user-uploaded gene/measurement sets.' Nucleic Acids Res. https://doi.org/10.1093/nar/gkab835

Taub DR, Miller B, Allen H (2008) Effects of elevated CO_2 on the protein concentration of food crops: a meta-analysis. Global Change Biol. https://doi.org/10.1111/j.1365-2486

Terhaag MM, Santos ACM, Lima DG et al (2025) Separation of bioactive compounds from *Pfaffia glomerata*: drying, green extraction, and physicochemical properties. Separations. https://doi.org/10.3390/separations12060164

Tsukagoshi Y, Ohyama K, Seki H et al (2016) Functional characterization of CYP71D443, a cytochrome P450 catalyzing C-22 hydroxylation in the 20-hydroxyecdysone biosynthesis of *Ajuga* hairy roots. Phytochemistry. https://doi.org/10.1016/j.phytochem.2016.03.010

Wang JP, Matthews ML, Williams CM et al (2018) Improving wood properties for wood utilization through multi-omics integration in lignin biosynthesis. Nat Commun. https://doi.org/10.1038/s41467-018-03863-z

Wang Z, Wang C, Liu S (2022) Elevated CO_2 alleviates adverse effects of drought on plant water relations and photosynthesis: a global meta-analysis. J Ecol. https://doi.org/10.1111/1365-2745.13988

Wu Y, Zhong H, Li J et al (2022) Water use efficiency and photosynthesis of *Calamagrostis angustifolia* leaves under drought stress through CO_2 concentration increase. J Plant Interact. https://doi.org/10.1080/17429145.2021.2011444

Xu Z, Jiang Y, Jia B et al (2016) Elevated-CO_2 response of stomata and its dependence on environmental factors. Front Plant Sci. https://doi.org/10.3389/fpls.2016.00657

Zhang X, Wang X , Zhuang L et al (2019) Abscisic acid mediation of drought priming-enhanced heat tolerance in tall fescue (*Festuca arundinacea*) and Arabidopsis. Physiol Plant. https://doi.org/10.1111/ppl.12975

Zhang L, Takahashi Y, Hsu P et al (2020) FRET kinase sensor development reveals SnRK2/OST1 activation by ABA but not by MeJA and high CO_2 during stomatal closure. eLife. https://doi.org/10.7554/eLife.56351

Publisher's Note Springer Nature remains neutral with regard to jurisdictional claims in published maps and institutional affiliations.

Authors and Affiliations

Tatiane Dulcineia Silva[1] · Evandro Alexandre Fortini[1] · Diego Silva Batista[2] · Kerly Jessenia Moncaleano Robledo[1] · Mariana Machado[1] · Sérgio Heitor Sousa Felipe[3] · Tadeu dos Reis de Oliveira[4] · Moab Torres de Andrade[1] · Letícia Monteiro Farias[5] · Claudete Santa-Catarina[4] · Vanildo Silveira[4] · Philipp Westhoff[6] · Andreas P. M. Weber[7] · Adriano Nunes-Nesi[1] · Wagner Campos Otoni[1]

✉ Wagner Campos Otoni
wotoni@ufv.br

Tatiane Dulcineia Silva
tatiane.silva.ufv@gmail.com

Evandro Alexandre Fortini
evandrofortini@gmail.com

Diego Silva Batista
diegoesperanca@gmail.com

Kerly Jessenia Moncaleano Robledo
kjmoncaleanor@unal.edu.com

Mariana Machado
mariana.f.machado@ufv.br

Sérgio Heitor Sousa Felipe
sergio.h.s.felipe@gmail.com

Tadeu dos Reis de Oliveira
tadeuoliveiraipu@gmail.com

Moab Torres de Andrade
moab.agro@gmail.com

Letícia Monteiro Farias
leticiamonteirofarias@hotmail.com

Claudete Santa-Catarina
claudete@uenf.br

Vanildo Silveira
vanildo@uenf.br

Philipp Westhoff
philipp.westhoff@hhu.de

Andreas P. M. Weber
aweber@hhu.de

Adriano Nunes-Nesi
nunesnesi@ufv.br

[1] National Institute of Science and Technology on Plant Physiology Under Stress Conditions, Departamento de Biologia Vegetal, Universidade Federal de Viçosa, Viçosa, MG 36570-900, Brazil

[2] Departamento de Agricultura, Universidade Federal da Paraíba, Bananeiras, Brazil

[3] Departamento de Engenharia Florestal, Universidade Federal Rural da Amazônia, Capitão Poço, Brazil

[4] Centro de Biociências e Biotecnologia, Universidade Estadual do Norte Fluminense Darcy Ribeiro, Campos Dos Goytacazes, Brazil

[5] Departamento de Bioquímica e Biologia Molecular, Universidade Federal de Viçosa, Viçosa, Brazil

[6] Plant Metabolism and Metabolomics Laboratory, Cluster of Excellence on Plant Sciences, Heinrich Heine University Düsseldorf, Düsseldorf, Germany

[7] Institute of Plant Biochemistry, Cluster of Excellence on Plant Science, Heinrich Heine University Düsseldorf, Düsseldorf, Germany